

Impact of Mechanical and Electrical Tilting for Cellular-Connected Drones and Legacy Users

by

Ahmad Elleathy

A thesis
presented to the University of Waterloo
in fulfillment of the
thesis requirement for the degree of
Master of Applied Science
in
Electrical and Computer Engineering

Waterloo, Ontario, Canada, 2024

© Ahmad Elleathy 2024

Author's Declaration

I hereby declare that I am the sole author of this thesis. This is a true copy of the thesis, including any required final revisions, as accepted by my examiners.

I understand that my thesis may be made electronically available to the public.

Abstract

Drones, also known as [Unmanned Aerial Vehicle \(UAV\)](#)s, have lately been employed for a variety of tasks in our daily lives, including surveillance, delivery, and rescue operations. High-performance, dependable two-way communication with cellular networks is necessary to expand [UAV](#) applications quickly. Supporting different [UAV](#)s into current [fifth generation \(5G\)](#) networks is challenging. One of these challenges comes from ground and aerial users having different channel properties. This thesis investigates how the performance of cellular-connected [UAV](#)s and legacy ground users in a cellular network can be improved by changing the antenna tilting angle or type, and we will consider mechanical, electrical, and hybrid tilting in the system. This study considers the case of [single user Multiple-Input Multiple-Output \(SU-MIMO\)](#) system featuring [Uniform Linear Array \(ULA\)](#) or [Uniform Planar Array \(UPA\)](#) antenna system with [Third Generation Partnership Project \(3GPP\)](#) parameters. This study illustrates the impact of antenna tilting in improving user throughput, making it easier to integrate [UAV](#)s into [5G](#) and future networks. These conclusions are supported by simulation results, which also show how hybrid tilting may be used as a scalable way to enhance multi-user performance for next-generation networks.

Acknowledgements

I thank Prof. Catherine Rosenberg and my colleague Ahmed El-Ashmawy for supporting my academic advancement and personal challenges. I couldn't have finished my thesis without their guidance and supervision. I am pleased and honored to be under their supervision, and the experience I have gained is precious for a lifetime.

I would like to thank my mother and father for their never-ending support and help every day. I am grateful to have wonderful parents, and my love for you cannot be expressed alone in words.

I'd like to thank the members of my MASc advising committee for reading my thesis and making constructive suggestions that improved its quality. I especially thank Prof. George Shaker for his insights regarding my work.

I want to thank my family and friends in Egypt, Saudi Arabia, and Canada for their support during my MASc studies. Your support has shaped me into a more optimistic and resilient individual. My special thanks to my friends and Professors from King Saud University in Saudi Arabia for their constant support. I am grateful to have friends in Waterloo for their assistance since my arrival in Canada.

I like to thank my lab mates, notably Abdalla Hussein, João Paulo, and Euan Quan, for all the fun and valuable talks we had over the years, and these memories I will cherish them.

Dedication

This is dedicated to the one I love.

Table of Contents

Author's Declaration	ii
Abstract	iii
Acknowledgements	iv
Dedication	v
List of Figures	ix
List of Tables	xii
List of Abbreviations	xiv
1 Introduction	1
1.1 Overview	1
1.2 Motivation	1
1.3 Contributions	3
1.4 Outline	4
2 Background and Literature Review	5
2.1 Background	5
2.1.1 Mechanical and electrical tilting effect on Antenna Gain	6

2.1.2	Difference between ULA and UPA systems	13
2.1.3	The effect of Hybrid tilting on the structure of the antenna	18
2.2	Related Work	19
3	Testing antenna tilt effect on ground users	21
3.1	Legacy Users' Settings	21
3.1.1	Pathloss	21
3.1.2	Channel setting	22
3.2	System Model and Parameters for SU-MIMO	24
3.2.1	Precoding and Calculating throughput	24
3.2.2	resource allocation	25
3.3	Mechanical and Electrical tilt in SU-MIMO	27
3.3.1	ULA antenna system with mechanical and electrical tilt	27
3.3.2	UPA antenna system with mechanical and electrical tilt	28
3.3.3	Difference between UPA and ULA in azimuth angle	31
3.4	Hybrid Tilting for Ground Users	32
3.4.1	Hybrid Tilting in ULA	32
3.4.2	Hybrid tilting in UPA	35
3.4.3	Hybrid tilting for ground users with ULA antenna system	38
3.4.4	Hybrid tilting for ground users with UPA antenna system	39
4	Integrating UAVs in a legacy system with antenna tilt effect	41
4.1	The importance of UAVs in a legacy network system	41
4.1.1	Types of UAVs	41
4.1.2	Applications of UAVs	42
4.1.3	The communication links of UAVs	45
4.1.4	Challenges for UAVs	45
4.2	Cellular-connected UAV's setting	46

4.3	Single-user MIMO with UAVs	47
4.3.1	Power and Antenna tilting angle	47
4.3.2	Number of users case and antenna tilting angle	49
4.3.3	Number of Antenna and antenna tilting angle	49
4.4	Hybrid Tilting for Cellular-connected UAVs	50
4.4.1	ULA system and Hybrid tilting	50
4.4.2	Optimal hybrid tilting angle with optimal realizations in ULA system	55
4.4.3	UPA system and hybrid tilting	57
4.4.4	Optimal hybrid tilting angle with optimal realizations in UPA system	61
5	Conclusions	63
	References	64

List of Figures

1.1	UAVs being served by side lobes	2
1.2	The system under the study	3
2.1	Elevation and azimuth angle representation in 3D	6
2.2	Untitled and Mechanically titled system	7
2.3	mechanical tilt on gain pattern	9
2.4	untitled and electrically tilted system	10
2.5	Electrical tilt on gain pattern	11
2.6	Distance vs Gain with different antenna tilt	12
2.7	ULA vs. UPA in 3D	13
2.8	ULA vs UPA	14
2.9	Vertical gain vs. elevation angle in UPA	16
2.10	Horizontal gain vs. azimuth angle in UPA	17
2.11	ULA Vs. UPA with 64 antenna elements in elevation angle	17
2.12	Gain(dB) vs Elevation Angle($^{\circ}$) in 3D	18
2.13	Mechanical up-tilt with electrical down-tilt	18
3.1	Pathloss vs distances	22
3.2	Throughput vs mechanical tilt in SU-MIMO	27
3.3	Throughput vs Electrical tilt in SU-MIMO	28
3.4	Throughput vs mechanical tilt in SU-MIMO in UPA system	29

3.5	Throughput vs Electrical tilt in SU-MIMO in UPA system	29
3.6	Location of the ground users in SU-MIMO with 20 ground users in UPA system	30
3.7	ULA Vs. UPA with 64 antenna elements in elevation angle at azimuth angle of 45°	31
3.8	ULA Vs. UPA with 64 antenna elements in elevation angle at azimuth angle of 90°	31
3.9	Gain(dB) vs Elevation Angle($^\circ$) with different tilting types at main beam	33
3.10	Gain(dB) vs Elevation Angle($^\circ$) with different tilting types at sidelobes	34
3.11	Gain(dB) vs Elevation Angle($^\circ$) with different tilting types	36
3.12	Gain(dB) vs Elevation Angle($^\circ$) with different tilting types at main beam	37
3.13	Gain(dB) vs Elevation Angle($^\circ$) with different tilting types at sidelobes in UPA	37
3.14	Throughput (bps) vs Hybrid tilt ($^\circ$) in ULA	38
3.15	Throughput (bps) vs Hybrid tilt ($^\circ$) in UPA	39
4.1	Different Applications of UAVs	43
4.2	Throughput (bps) Vs Antenna tilt angles (degree) for 100 realizations with BS power of 0.1 W	48
4.3	Throughput (bps) Vs Antenna tilt angles (degree) for 100 realizations with BS power of 1 W	48
4.4	Throughput (bps) Vs Antenna tilt angles (degree) for 100 realizations with BS power of 40 W	48
4.5	Throughput (bps) Vs Mechanical Antenna tilt angles (degree) vs electrical tilt (degree) for 20 ground User Equipment (UE)s	51
4.6	Throughput (bps) Vs Mechanical Antenna tilt angles (degree) vs electrical tilt (degree) for 20 UAVs	51
4.7	Throughput (bps) Vs Mechanical Antenna tilt angles (degree) vs electrical tilt (degree) for 20 ground UEs with threshold	52
4.8	Throughput (bps) Vs Mechanical Antenna tilt angles (degree) vs electrical tilt (degree) for 20 ground UEs and 20 UAVs combined	52

4.9	Location of the ground users in SU-MIMO with 20 ground users and 20 UAVs in ULA system	53
4.10	Common Tilting angle across different realizations between 500 and 1000	55
4.11	Throughput (bps) Vs Mechanical Antenna tilt angles (degree) vs electrical tilt (degree) for 20 ground UEs	58
4.12	Throughput (bps) Vs Mechanical Antenna tilt angles (degree) vs electrical tilt (degree) for 20 UAVs	58
4.13	Throughput (bps) Vs Mechanical Antenna tilt angles (degree) vs electrical tilt (degree) for 40 UEs	59
4.14	Throughput (bps) Vs Mechanical Antenna tilt angles (degree) vs electrical tilt (degree) for 20 UEs ground users with threshold	60

List of Tables

2.1	Comparison of mechanical, electrical, and hybrid tilt with array factor gain and cellular-connected UAVs in Literature and our Research	20
3.1	Parameters under downlink case	24
3.2	Optimal tilting angles for the geometric mean of ground users' throughput	39
3.3	Optimal tilting angles for geometric mean of ground users' throughput (Mbps) in UPA antenna system	40
4.1	Different power cases of 0.1,1, and 40W for 20 users with corresponding best tilting angle	47
4.2	Different numbers of users such as 20,40, and 60 at 0.1 W with corresponding best tilting angle.	49
4.3	60 User with different numbers of antennas such as 32 and 64 at 0.1 W with corresponding best tilting angle	49
4.4	Best antenna hybrid tilt angles for different users in ULA	50
4.5	Best hybrid tilting angles for ground UEs with UAVs' throughput in ULA system	54
4.6	Best hybrid angles and their respective realizations from 20 to 1000	55
4.7	UAV's and ground Users' throughput at different optimal down-tilted angles for 550 realizations in ULA system	56
4.8	Best antenna hybrid tilt angles for different users in UPA	57
4.9	Best antenna hybrid tilt angles for different users in UPA with azimuth angle of 0°	60

4.10 Best tilting angles and their Respective realizations from 550 to 850	61
4.11 Optimal electrical and mechanical tilt angles with 650 realizations in UPA system	62

List of Abbreviations

3GPP Third Generation Partnership Project [iii](#), [2](#), [3](#), [5](#), [7](#), [15](#), [16](#), [19](#), [21](#), [22](#), [32](#), [35](#), [46](#)

4G fourth generation [25](#)

5G fifth generation [iii](#), [1](#), [2](#), [25](#)

6G sixth generation [1](#)

ATA antenna tilt angle [2–4](#), [18](#), [19](#)

BS Base Station [1](#), [2](#), [5](#), [7](#), [10](#), [12](#), [19](#), [24](#), [25](#), [32](#), [42–45](#), [47](#), [49](#), [63](#)

EMA Exponential Moving Average [25](#), [26](#), [47](#)

FAA Federal Aviation Administration [1](#)

HAPs High altitude platforms [42](#)

HPBW Half-Power Beamwidth [7](#)

IoT Internet of Things [1](#)

LAPs Low altitude platforms [42](#)

LOS Line of Sight [1](#), [2](#), [5](#), [22](#), [42](#), [44–47](#)

MCS Modulation Coding Scheme [25](#), [26](#), [47](#)

MRT Maximal Ratio Transmission [24](#), [25](#)

MU-MIMO Multi user Multiple-Input Multiple-Output 24, 63

OFDMA Orthogonal Frequency Division Multiple Access 25

PRB Physical Resource Block 25, 47

QOS Quality-of-Service 45

RF Radio frequency 5

SAR Search and Rescue 42–44

SINR Signal-to-Interference-plus-Noise Ratio 24–26, 45

SU-MIMO single user Multiple-Input Multiple-Output iii, 3, 24–27, 32, 38, 41, 47, 49

UAV Unmanned Aerial Vehicle iii, x, xi, 1–6, 19, 20, 34, 41–47, 49–51, 53, 55–58, 60, 61, 63

UE User Equipment x, xi, 1–3, 5, 19, 24, 25, 34, 44, 46, 47, 50–52, 55, 56, 58, 60

ULA Uniform Linear Array iii, ix, 3, 5, 6, 10, 13, 14, 16, 17, 19, 21, 23, 27, 28, 31, 32, 35, 37–39, 47, 50, 57, 63

UMa urban macrocell 3, 21, 46

UPA Uniform Planar Array iii, ix, 3, 5, 6, 13–21, 23, 27, 28, 30–32, 35–37, 39, 57, 60, 61, 63

Chapter 1

Introduction

1.1 Overview

The use of [Unmanned Aerial Vehicle \(UAV\)](#)s, popularly known as drones, has grown in the last decade. Drones have specific features that make them helpful technology, such as changeable altitude, flexibility, mobility, and reliability. Moreover, [UAVs](#) have new and diverse applications with great business opportunities [1]. According to a report by [Federal Aviation Administration \(FAA\)](#), drones are expected to reach approximately 1.8 million by 2027 [2]. [UAV](#) plays a role in [5G](#) and [sixth generation \(6G\)](#) wireless systems, in which drones can be used as aerial [Base Station \(BS\)](#) for energy harvesting or edge computing [3]. Drones can also be used as nodes or relays in ad hoc networks, where these relays can be used between the ground [BS](#) and [UAVs](#) [4]. Finally, drones can be users of a cellular system, and this is the focus of this thesis.

1.2 Motivation

Cellular-connected drones coexist with ground [UEs](#) in a cellular network [5]. They can be used as part of [Internet of Things \(IoT\)](#) devices or sensors due to their small range and power [5]. Drones, or [UAVs](#), are increasingly being integrated into wireless communication networks because they are low-cost mobile aerial vehicles and have a high probability or chance of maintaining a [Line of Sight \(LOS\)](#) connection [6]. Many telecommunication operators do not disclose their antenna configurations. More investigations are needed regarding different antenna tilting types and angles to enhance the overall system's

throughput. Some UAV often connect to a farther BS rather than a closer one due to the high power or high LOS probability of the sidelobes¹ of the distant BS [7] as shown in figure 1.1. This shows that antenna tilt angle (ATA) might be useful for association, and interference between ground users and drones in some cases. Moreover, this approach can help maintain better performance in a 5G network [8]. We will use ATA and its different types to observe its effect and performance on the system.

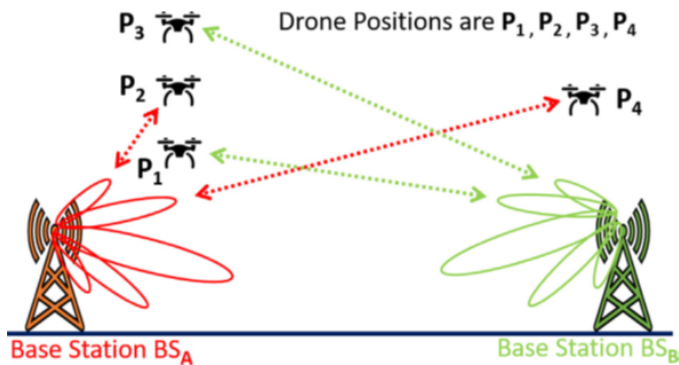


Figure 1.1: UAVs being served by side lobes (adapted from [9])

This study relies on the 3GPP specifications to find the performance for both UAVs and ground UEs. The main questions of this research are:

- How much flexibility do we have with down-tilted antenna angles from the standpoint of the legacy users?
- How can this flexibility be used to improve the performance of UAVs?

¹Sidelobes are the side emissions of an antenna’s radiation pattern, which can cause interference and affect signal strength in unintended directions. Secondary lobes are also sidelobes

The antenna configurations have a significant impact on throughput and user coverage in real-life scenarios. Figure 1.2 illustrates how tilting can offer the edge users some fairness and shows the importance of using BS antenna tilting for different types of UEs in a system, and it represents the system for this study. We used a single urban macrocell (UMa) environment based on 3GPP parameters with SU-MIMO scheduling focusing on the downlink.

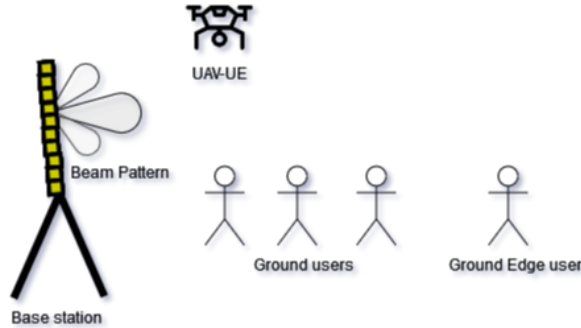


Figure 1.2: The system under the study

1.3 Contributions

The main contributions are:

1. The effect of ATA on a ULA and UPA antenna systems.
2. Hybrid tilting offers better gain for sidelobes in ULA and UPA systems than mechanical and electrical tilting.
3. Hybrid tilting increases the UAVs' throughput for down-tilted antenna while maintaining equal or greater than 95% of the maximum throughput for the legacy UEs.

1.4 Outline

Chapter 2 shows the background and related work in antenna tilting. Chapter 3 displays how tilting can affect the performance of the legacy users in a system, while Chapter 4 integrates UAVs into the legacy system. Lastly, Chapter 5 summarizes the research findings and raises questions regarding ATA for future work.

Chapter 2

Background and Literature Review

2.1 Background

Integrating the Cellular-connected UAVs in legacy networks creates unique challenges, including increased interference due to their high probability of LOS [7]. Therefore, antenna tilting is one of the practical approaches that effectively enhances signal coverage and reduces interference for UAVs and ground users. Tilting is one of the important parameters for a BS as it impacts the coverage and interference for the legacy network. In any legacy system, the BS has down-tilted antennas for ground users to have high throughput and connectivity. Tilting the BS's antenna can help decrease interference and handover between ground UEs and drones [10], and it can provide better and fairer performance for edge users in the system. Tilting can be of three types: mechanical, electrical, and hybrid tilting [11]. This study will combine mechanical and electrical tilting as hybrid tilting. Many telecommunication vendors don't disclose their antenna parameters or Radio frequency (RF) configurations, and this causes ambiguity for researchers in finding a better way to enhance the performance of the legacy systems or allow the integration of any new technology into the legacy systems effectively. Mechanical tilt is achieved by changing the physical attributes or position of the antenna at the BS, while electrical tilt can be done remotely by the network operator [12]. Tilting is different in ULA and UPA systems, as ULA would have more sidelobes than a UPA system if both systems have the same number of element antennas. Integrating cellular-connected UAVs into a legacy system with down-tilted antennas would be a challenge, as UAVs has great LOS probability based on the 3GPP model [13] and associate with further BS as mentioned in section 1.2. Furthermore, another challenge is getting the optimal angles that offer 95% of the maximum throughput

of the ground users and provide better performance for UAV in the system. This Chapter will discuss electrical and mechanical tilt in more detail and the difference between ULA and UPA in terms of gain.

2.1.1 Mechanical and electrical tilting effect on Antenna Gain

This section will show the impact of mechanical and electrical tilt using gain equations. Figure 2.1 shows the elevation angle as θ and the azimuth angle as ϕ , where we will apply mechanical and electrical tilt angle on the elevation angle θ .

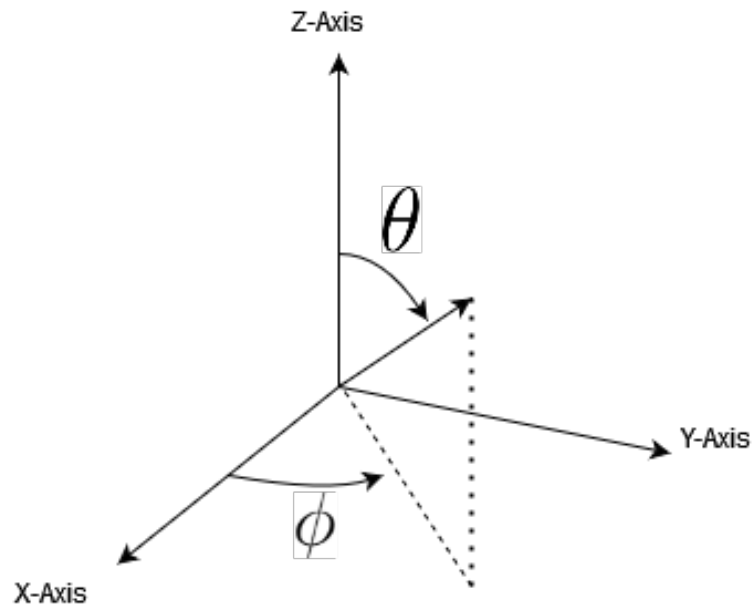


Figure 2.1: Elevation and azimuth angle representation in 3D

Mechanical tilting on the antenna gain

Mechanical tilt requires a change of the antenna's position along the Z-axis of the BS, where the antenna is physically rotated. In this study, changing the elevation angle of the BS's antenna is considered a mechanical tilt. Figure 2.2 shows how tilting is applied to the antenna of the BS:

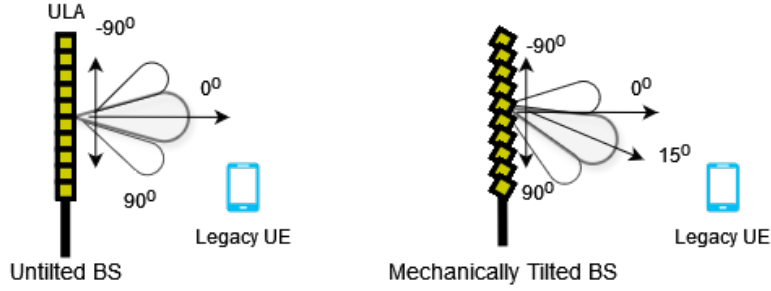


Figure 2.2: Untilted and Mechanically titled system

The vertical mechanical tilt angle for the antenna element is denoted as θ_m , influencing the gain of the antenna element in the vertical plane. The power (in dB) of the antenna element gain pattern, based on 3GPP specifications [14], is given by:

$$G_{E,V} = - \min \left(12 \left(\frac{\theta - \theta_m}{HPBW_v} \right)^2, G_m \right) \quad (2.1)$$

Where:

- $G_{E,V}$ represents the gain in the vertical plane for a given elevation angle θ .
- θ is the elevation angle of the incoming signal, varying from $[-90^\circ, 90^\circ]$.
- $HPBW_v$ is the vertical Half Power Beamwidth (**Half-Power Beamwidth (HPBW)**).
- G_m is the overall sidelobe level in vertical plane set by 3GPP specifications.

The elevation angle θ at each user is determined by the relative positions of the Base Station (BS) and the User Equipment (UE) and can be calculated as:

$$\theta = \arctan \left(\frac{H_{\text{BS}} - H_{\text{UE}}}{\sqrt{(X_{\text{UE}} - X_{\text{BS}})^2 + (Y_{\text{UE}} - Y_{\text{BS}})^2}} \right) \quad (2.2)$$

In this formula:

- H_{BS} and H_{UE} are the heights of the BS and UE in the Z-axis,
- X_{UE} and Y_{UE} represent the horizontal coordinates of the UE in the X-axis and Y-axis, respectively.
- X_{BS} and Y_{BS} represent the horizontal coordinates of the BS in the X-axis and Y-axis, respectively.

N represents the number of antenna elements for the vertical array factor. In this study, we will assume that N antennas are uniformly spaced with a separation of half the wavelength for every array factor, where $d = \frac{\lambda}{2}$ represents the distance between adjacent elements and $k = \frac{2\pi}{\lambda}$ represents the wave-number. This assumption simplifies the vertical array factor $\text{AF}_V(\theta)$ as shown in equation 2.3. The mechanical tilt angle of the array is denoted as θ_m . Given these parameters, the array factor for N antennas with mechanical tilt θ_m is expressed as:

$$\text{AF}_V(\theta) = \sum_{n=0}^{N-1} e^{jnkd \sin(\theta - \theta_m)} = \frac{1}{\sqrt{N}} \frac{\sin \left(\frac{N\pi}{2} \sin(\theta - \theta_m) \right)}{\sin \left(\frac{\pi}{2} \sin(\theta - \theta_m) \right)}, \quad (2.3)$$

This formulation of $\text{AF}_V(\theta)$ provides the relative amplitude and phase pattern of the antenna array, illustrating how the vertical beam is shaped and directed by adjusting θ_m for better coverage and interference control. To get the power array factor in dB scale, let's calculate it as:

$$G_{F,V}(\theta) \triangleq 10 \log_{10} (\text{AF}_V(\theta))^2 \quad (2.4)$$

The overall Gain that consists of the element gain and array factor of the antenna can be represented as:

$$G_V(\theta) = G_{E,V}(\theta) + G_{F,V}(\theta) \quad (2.5)$$

Based on the figure 2.3, mechanical tilt shifts the same gain beam to a tilting angle without changing the beam pattern shape or features itself, and the user that's located at elevation angle 15° would receive the highest Gain or the main beam gain.

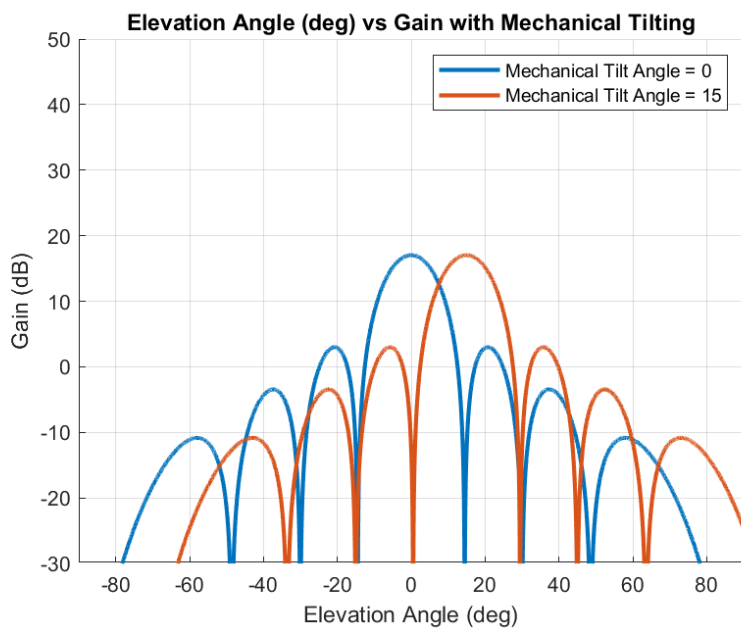


Figure 2.3: mechanical tilt on gain pattern

Electrical tilt on the antenna gain

Unlike mechanical tilting, electrical tilting uses the same element gain and array factor equations, except the beam steering angle is added to the array factor as $\sin(\theta_e)$ as shown in equation 2.7. The electrical tilt applied to a BS system doesn't physically affect the position or the axis of the antenna, as shown in figure 2.4.

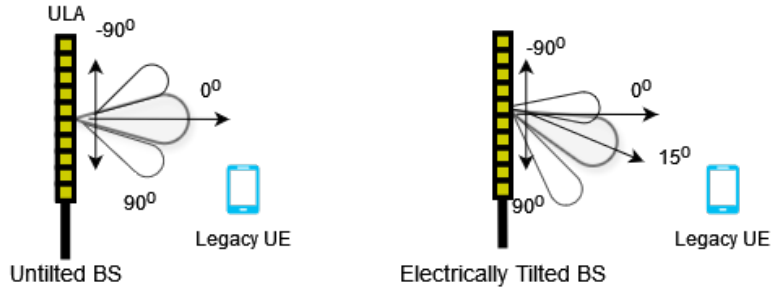


Figure 2.4: untitled and electrically tilted system

Equation 2.6 shows the element gain power (in dB) for a vertical ULA system can be represented as:

$$G_{E,V}(\theta) = -\min \left(12 \left(\frac{\theta}{HPBW_v} \right)^2, G_m \right) \quad (2.6)$$

Since the angle $\theta \in [-90^\circ, 90^\circ]$, and the vertical array factor from [15] in a ULA with the electrical tilt angle or beam steering angle as θ_e can be given as:

$$AF_V(\theta) = \sum_{n=0}^{N-1} e^{jnk d(\sin(\theta) - \sin(\theta_e))} = \frac{1}{\sqrt{N}} \frac{\sin \left(\frac{N\pi}{2} (\sin(\theta) - \sin(\theta_e)) \right)}{\sin \left(\frac{\pi}{2} (\sin(\theta) - \sin(\theta_e)) \right)} \quad (2.7)$$

Since electrical tilt changes the phase of the array, the beam pattern would not be symmetrical in shape as the same mechanical tilt's beam pattern as shown in figure 2.5.

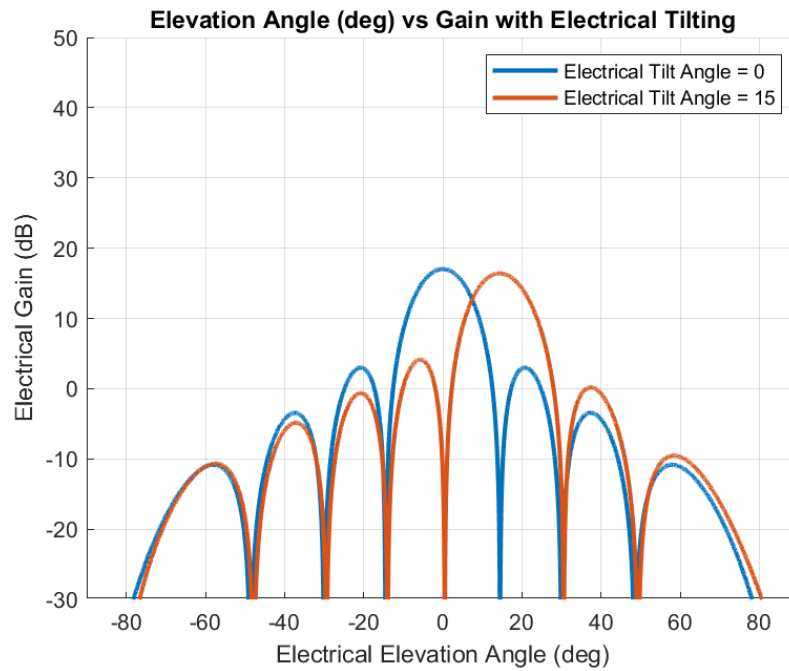


Figure 2.5: Electrical tilt on gain pattern

Side lobes problem

Since the system's Gain has an array factor, we should consider that some tilts might be better than others because of the sidelobe effect. Figure 2.6 shows how the different mechanical tilts affect the sidelobes at various distances away from the BS and how different antenna tilt angles are better than others at specific distances.

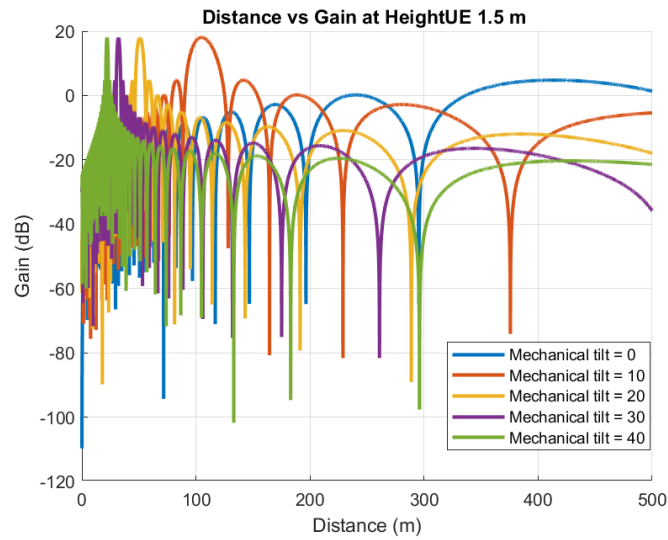


Figure 2.6: Distance vs Gain with different antenna tilt

2.1.2 Difference between ULA and UPA systems

The main difference between UPA and ULA system is that UPA system consists of horizontal and vertical gain, while ULA consists of vertical gain only [15]. In a ULA, the number of antenna elements is arranged linearly, with a total of N elements along a single dimension, resulting in an array size of $N \times 1$ or $1 \times N$. This structure allows the ULA to focus its beam in a single spatial direction, typically along the azimuth plane. Figure 2.7 shows the difference between two ULA systems and a single UPA system in terms of beam pattern, and it shows the gain pattern for ULA and UPA systems with eight and 8×8 elements, respectively.

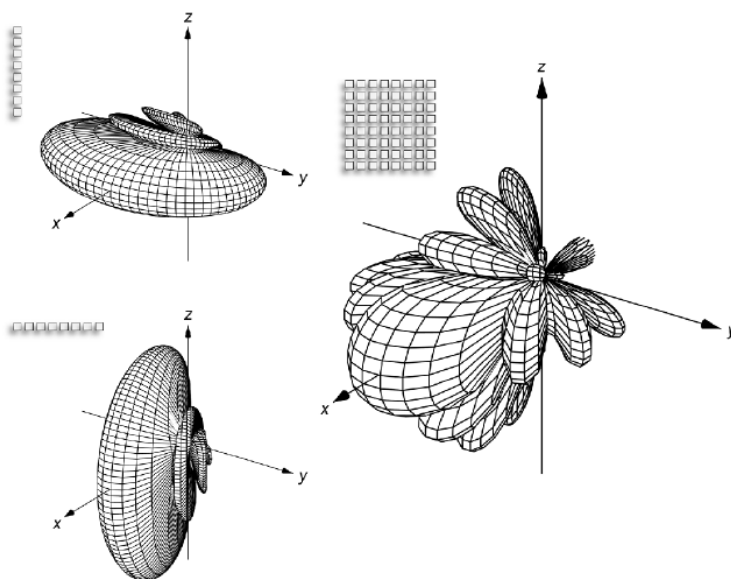


Figure 2.7: ULA vs. UPA in 3D (adapted from [15])

On the other hand, a UPA system arranges the elements in two dimensions, with N_1 elements along one axis and N_2 elements along the orthogonal axis. The total number of elements in a UPA is therefore given by $N = N_1 \times N_2$. This two-dimensional structure allows the UPA to achieve beamforming capabilities in both the azimuth and elevation planes, and it is more directive than the ULA antenna system. Figure 2.8 shows the structural difference between ULA and UPA system and how UPA antenna system is much larger than ULA antenna system.

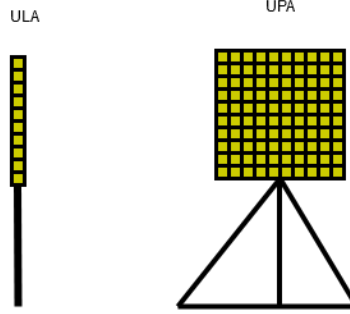


Figure 2.8: ULA vs UPA

To compute the horizontal gain, the azimuth angle, ϕ , is calculated based on the relative positions of the base station (BS) and the user equipment (UE), as shown in Equation 2.8:

$$\phi = \arctan \left(\frac{Y_{\text{UE}} - Y_{\text{BS}}}{X_{\text{UE}} - X_{\text{BS}}} \right) \quad (2.8)$$

In this equation:

- ϕ represents the azimuth angle between the BS and the UE, measured in radians.
- Y_{UE} and X_{UE} are the coordinates of the UE in the Y-axis and X-axis, respectively.
- Y_{BS} and X_{BS} are the coordinates of the BS in the Y-axis and X-axis, respectively.

The azimuth angle ϕ provides the angular direction from the BS to the UE, essential for determining the horizontal gain in antenna alignment.

The gain element and array factor for the horizontal cut of the radiation pattern characterize the power distribution across the horizontal plane. Each antenna component's gain can be expressed as in Equation 2.9, defined in terms of the horizontal dimension. For the horizontal cut gain, the azimuth angle ϕ varies within a range of $[-90^\circ, 90^\circ]$. The array factor follows the same form as the vertical ULA, replacing the elevation angle with the azimuth angle. Equation 2.9 describes the gain pattern regarding the azimuth angle and horizontal plane.

$$G_{E,H}(\phi) = -\min \left\{ 12 \left(\frac{\phi}{\text{HPBW}_h} \right)^2, A_m \right\}, \quad \text{HPBW}_h = 65^\circ, \quad A_m = 30 \text{ dB} \quad (2.9)$$

In equation 2.9:

- $G_{E,H}(\phi)$ is the horizontal gain component of the antenna radiation pattern at an azimuth angle ϕ .
- ϕ is the azimuth angle, representing the horizontal direction of the incoming wave, measured relative to the boresight direction of the antenna.
- $A_m = 30$ dB is overall sidelobes level for the horizontal element gain from 3GPP [14].
- $HPBW_h = 65^\circ$ denotes the half-power (3 dB) beamwidth in the horizontal plane, according to 3GPP standard [14].

For the horizontal array factor, N_h represents the number of antenna elements for the array factor equation in 2.10. Since we are not focusing on beam steering or electrical tilt for the horizontal part in the UPA antenna system, the horizontal array factor gain can be represented with the same considerations as in equation 2.3 as [15]:

$$AF_h(\theta, \varphi) = \frac{1}{\sqrt{N_h}} \sum_{n=0}^{N_h-1} e^{jkd_h n \cos(\theta - \theta_m) \sin \varphi} = \frac{1}{\sqrt{N_h}} \frac{\sin\left(\frac{N\pi}{2} \sin \varphi \cos(\theta)\right)}{\sin\left(\frac{\pi}{2} \sin \varphi \cos(\theta)\right)} \quad (2.10)$$

If we want to add vertical mechanical tilt, the only factor influencing the horizontal array factor gain and Gain element is the elevation angle θ , which will be adjusted to $\theta - \theta_m$. The final antenna element gain with vertical and horizontal Gain in UPA can be calculated as :

$$Ge(\theta, \phi) = - \min \{ - (G_{E,V}(\theta) + G_{E,H}(\phi)), G_m \} \quad (2.11)$$

Where:

- $Ge(\theta, \phi)$ is the total antenna element gain in both the vertical and horizontal planes.
- $G_{E,V}(\theta)$ is the vertical gain component based on the elevation angle θ .
- $G_{E,H}(\phi)$ is the horizontal gain component based on the azimuth angle ϕ .
- G_m is the maximum sidelobe level, limiting the combined gain as per system specifications from [3GPP](#).

The total Gain, incorporating both vertical and horizontal gains in terms of the element gain and array factors, can be expressed as:

$$G_{\text{total}}(\theta, \phi) = 8 - Ge(\theta, \phi) + 10 \log_{10} ((AF_v(\theta))^2 (AF_h(\phi))^2) \quad (2.12)$$

Since [UPA](#) consists of horizontal and vertical gain, this means the gains can be represented similarly to [ULA](#) in polar form with a mechanical vertical tilt of 10° as shown in figures [2.9](#) and [2.10](#) [[14](#)]. Figure [2.9](#) shows the gain pattern as a function of elevation angle (θ) for azimuth angle (ϕ) equal to zero, and Figure [2.10](#) shows the gain pattern as a function of azimuth angle (ϕ) for elevation angle (θ) equal to zero.

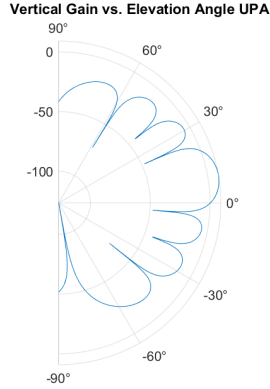


Figure 2.9: Vertical gain vs. elevation angle in UPA

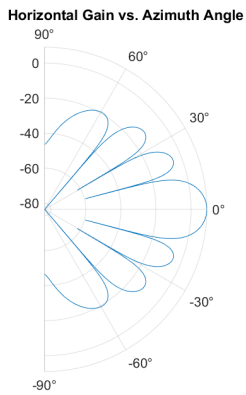


Figure 2.10: Horizontal gain vs. azimuth angle in UPA

Difference between UPA and ULA in terms of Gain

UPA has fewer sidelobes than ULA has because UPA has better beam control in azimuth and elevation plane. Figure 2.11 provides the difference between ULA and UPA in terms of antenna gain pattern at azimuth angle of 0° :

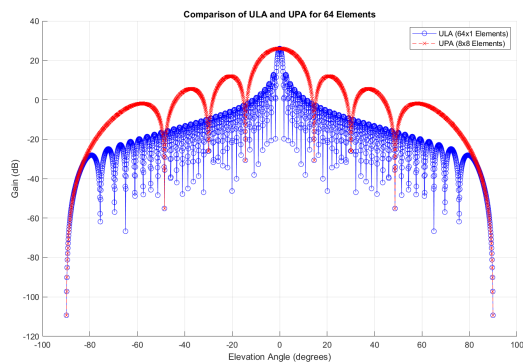


Figure 2.11: ULA Vs. UPA with 64 antenna elements in elevation angle

UPA in 3D

We can also represent UPA in 3D since UPA has azimuth and elevation planes. Figure 2.12 shows a UPA system in 3D.

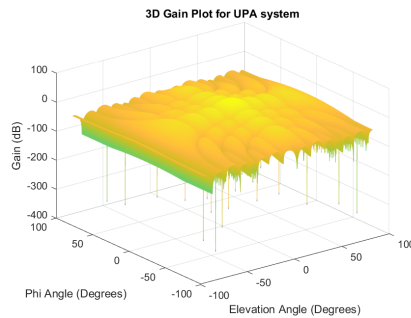


Figure 2.12: Gain(dB) vs Elevation Angle(°) in 3D

2.1.3 The effect of Hybrid tilting on the structure of the antenna

In a hybrid tilting system, we use electrical and mechanical ATA simultaneously, in which both angles are separate angles that are not added into one angle. Figure 2.13 shows how we can add mechanical tilt to change the position of the antenna, and we can also add electrical tilt to steer the beam in a specific way by changing the phases of the antennas.

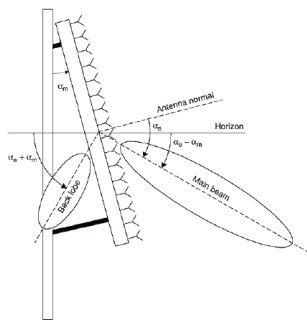


Figure 2.13: Mechanical up-tilt with electrical down-tilt (adapted from [11])

2.2 Related Work

There is some lack of considerable representation of Gain in the current literature. The electrical and mechanical tilt was not clear in 3GPP for UAVs and ground users in the same system, and the Gain of the array factor gain is not well considered in [16]. Based on 3GPP specification in [14], the standard electrical tilt for BS is 12° for ground users, but the mechanical tilt standard was not considered. Many studies covered the effect of mechanical and electrical tilt on legacy users. However, the representation of mechanical and electrical tilting was not well established in some studies because array factor gain was not taken into consideration, and this can be found in [12],[17], and [18]. Therefore, this causes the gain pattern to not have sidelobes, while other ULA systems in the literature have sidelobes because of adding the antenna array factor to the gain element.

An essential aspect of tilting that wasn't well illustrated in some of the literature is Hybrid or combined tilting. The impact and use of Hybrid tilting were taken as an equal amount of electrical and mechanical tilt in [12]. However, we will use different amounts or combinations of electrical and mechanical tilt in this thesis. Some studies recently, such as [19, 20] focused on the use of electrical tilting for cellular-connected UAVs in a legacy system. Moreover, the authors in [7] considered using mechanical tilting with 12° instead of electrical tilting for cellular-connected UAVs. Using different combinations of electrical and mechanical tilting angles for cellular-connected UAVs and ground UE in a legacy system was not used before. Our wireless network system in this study has a channel for every user with scheduling based on the user's weight, while the system in [19] uses the Gain directly without implementing it in the channel. Many works such as [19, 21] use up-tilted antennas specifically for cellular-connected UAVs, which it is not cost-efficient to have each special antenna in each BS for a few aerial users that are far less than ground UEs, and up-tilted antennas can affect airplanes in the surrounding area. In [20], the authors used ULA and UPA for cellular-connected UAVs and ground users. However, they didn't specify the tilting type in the element gain or the array factor equations in the clear matter.

This study takes careful consideration antenna gain model and clearly distinguishes between electrical and mechanical tilting, as shown in the background. We will use tilting to enhance performance for UAVs while emphasizing the importance of maintaining ground UEs throughput. We will employ separate mechanical and electrical tilting angles using distinct ATA configurations rather than combining them into a single ATA, as has been done in some previous studies [18].

Table 2.1 summarizes how this thesis covers essential aspects that are not found in many studies, such as antenna gain representation with array factor gain, cellular-connected UAVs, electrical tilting, mechanical tilting, and UPA antenna system.

Table 2.1: Comparison of mechanical, electrical, and hybrid tilt with array factor gain and cellular-connected UAVs in Literature and our Research

Reference	Mechanical Tilt	Electrical Tilt	Hybrid Tilt	Array Factor Gain	Cellular-Connected UAVs	UPA Antenna Gain
Geraci et al. (2018) [7]	✓	X	X	✓	✓	✓
Yilmaz et al. (2009) [16]	✓	✓	X	X	X	✓
3GPP [13, 14]	X	✓	X	X	✓	✓
Athley and Johansson (2010) [12]	✓	✓	✓ (Equal Tilt)	X	X	✓
Seifi et al. (2012) [17]	✓	✓	X	X	X	✓
Dandanov et al. (2017) [18]	✓	✓	X	X	X	✓
Chowdhury et al. (2021) [19]	X	✓	X	✓	✓	X
Lobão et al. (2023) [20]	X	✓	X	✓	✓	✓
Du et al. (2022) [21]	X	✓	X	✓	✓	X
Kim et al. (2020) [22]	✓	✓	X	X	✓	X
Xu and Zeng (2019) [23]	X	✓	X	X	✓	X
Our Research	✓	✓	✓ (Custom Combinations)	✓	✓	✓

Chapter 3

Testing antenna tilt effect on ground users

In this chapter, we will show the impact of antenna tilt angle on ground users in legacy systems. The following section 3.1 shows the system's parameters. Our central antenna system would be [ULA](#) with a downlink case, but we will also illustrate a case with [UPA](#). Mechanical, electrical, and hybrid tilting for ground users will be shown in this chapter.

3.1 Legacy Users' Settings

3.1.1 Pathloss

In this work, we will use [3GPP](#) specifications for ground users from [14]. [UMa](#) was considered in the system. In figure 3.1, we simulated the different Pathloss cases with distance to understand the relationship between Pathloss and distance for ground users.

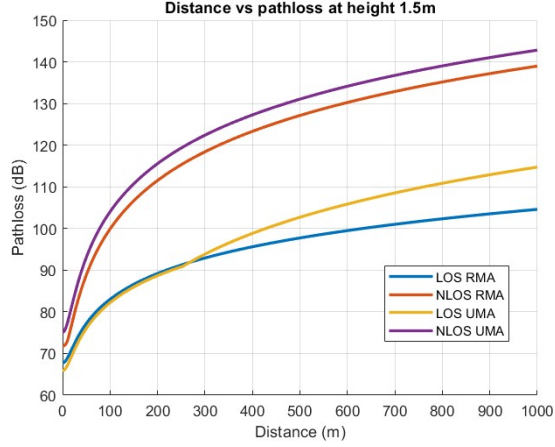


Figure 3.1: Pathloss vs distances

3.1.2 Channel setting

The Rician fading model equation can be written as:

$$\mathbf{g}_k^n = \sqrt{\frac{\beta_k^n}{1 + \kappa_k^n}} \mathbf{h}_G^n \mathbf{R}^{\frac{1}{2}} + \sqrt{\frac{\kappa_k^n \beta_k^n}{1 + \kappa_k^n}} \mathbf{h}_k^{\text{LOS},n} \quad (3.1)$$

Users with **LOS** components in the system use the Rician fading model, while others use the Rayleigh fading model. Based on equation (3.1), we have β_k^n that is assumed to be the LOS coefficient for the first tap, and the rest of the taps are assumed to be NLOS coefficients. In addition, each tapped delay-line has its own power delay profile based on **3GPP** specifications [14]. κ_k^n is the Rician factor, where κ -th is the number of users at the n -th time-slot. $\mathbf{h}_k^{\text{LOS},n}$ represents the LOS components, where it is zero for the Rayleigh fading model. The transmit antenna correlation matrix for users and the BS is shown as $\mathbf{R}^{1/2}$, and the \mathbf{h}_G^n is the vector whose entries are zero-mean i.i.d complex Gaussian random variables. The Rayleigh fading model is the Rician fading model without the dominant LOS component, so the LOS component and Rician factor will be zero in this case. In this step, we use the pathloss of LOS components in the channel matrix equation. However, we need to know whether the condition is LOS or NLOS depending on the probability of LOS. The likelihood of the LOS equation is based on 3GPP Rel 16 [14]. The equation used for the LOS probability can be described as follows:

$$\begin{aligned} & \text{Pr}_{\text{LOS,UMa}}^{k,n} \\ &= \begin{cases} 1, & d_{2D}^{k,n} \leq 18 \text{ m}; \\ \frac{18}{d_{2D}^{k,n}} + \exp\left(-\frac{d_{2D}^{k,n}}{63}\right) \left(1 - \frac{18}{d_{2D}^{k,n}}\right), & 18 \text{ m} < d_{2D}^{k,n}, \end{cases} \end{aligned} \quad (3.2)$$

The Line-of-Sight (LOS) channel component between the k -th User Equipment (UE) and the m -th antenna of the Base Station (BS) at the n -th time-slot is mathematically expressed as:

$$h_{k,m}^{\text{LOS},n} = e^{j\frac{2\pi}{\lambda} \|\mathbf{u}_k^n - \mathbf{a}_m\|_2}, \quad (3.3)$$

where:

- $\|\mathbf{u}_k^n - \mathbf{a}_m\|_2$ is the Euclidean distance between the k -th UE's position \mathbf{u}_k^n and the m -th antenna's position \mathbf{a}_m ,
- λ is the signal wavelength, defined as $\lambda = \frac{c}{f_c}$, where c is the speed of light, and f_c is the carrier frequency.

This equation captures the phase shift induced by the direct LOS path between the user and the antenna.

The base station (BS) can be equipped with either a [ULA](#) or a [UPA](#). The antenna elements are arranged linearly in the ULA, while in the UPA, they are placed in both vertical and horizontal directions, with identical spacing d . For the UPA, there are \sqrt{M} elements in each direction [24]. An exponential correlation model is used to capture the spatial correlation between the elements for both ULA and UPA, as described in [25]. The correlation matrix \mathbf{R} , with the (i, j) -th entry given by:

$$[\mathbf{R}]_{i,j} = \rho^{|v(i)-v(j)|+|h(i)-h(j)|}, \quad i, j = 1, 2, \dots, M \quad (3.4)$$

In the ULA, $v(i)$ refers to the position along the linear array, while for the UPA, $v(i)$ and $h(i)$ represent vertical and horizontal positions. The parameter ρ describes the correlation coefficient.

3.2 System Model and Parameters for SU-MIMO

This section will define our system's parameters for legacy users in the downlink scenario with SU-MIMO system. Table 3.1 represents the parameters set in this system, and some parameters are from 3GPP [14].

Table 3.1: Parameters under downlink case

Parameters	Values under Downlink Case
The carrier frequency (f_c)	2GHz
The system bandwidth (B)	20MHz
Total antennas at BS (M_{BS})	{64}
The average building height (d_b)	5m
The average street width (d_s)	20m
The minimum distance from the BS (d_{min}^{2D})	10m
The power density of noise (N_0)	-174dBm/Hz
The noise figure (ζ)	9dB
The effective antenna height at the BS (d_{BS})	25m
The effective antenna height at the user (d_{UE})	1.5m
The adjacent antenna distance at BS (d)	0.5λ
The adjacent antenna distance at UE (d)	0.2
The Rician factor (κ)	$\mathcal{N}(9, 3.5^2)$ dB
The BS channel correlation coefficient (ρ)	0.4
The maximum power of the BS (P_{max})	{0.1} W
The maximum height for UAVs ($Height_{UAV}$)	100m
Environment parameters for Rician factor (λ_1, λ_2)	1, 0.7329
Number of sub-channels (C)	{51}
Cell radius (\mathcal{R})	288m
Subchannel bandwidth (B_C)	360kHz
Number of time-slots per frame (T)	{20}
Time-slot duration (T_s)	0.5 ms

3.2.1 Precoding and Calculating throughput

The Signal-to-Interference-plus-Noise Ratio (SINR) for the κ -th user in a SU-MIMO system at the η -th timeslot using Maximal Ratio Transmission (MRT) is given by equation 3.5. MRT is a method of digital beamforming used to increase the maximal power at the receiver by changing the phase and amplitude of the transmitted signals. Moreover, It achieves this by aligning the signal in the same direction as the channel's complex conjugate. In this equation, $SINR_{\kappa}^{\eta}$ represents the SINR of the κ -th user at timeslot η , where P_{κ}^{η} denotes the transmit power, $\mathbf{h}_{\kappa}^{\eta}$ is the channel vector between the BS and the UE, and $\mathbf{w}_{\kappa}^{\eta}$ is the beamforming vector for the κ -th user. The term σ^2 , representing the noise power, is assumed to be 1. Unlike Multi user Multiple-Input Multiple-Output (MU-MIMO), SU-MIMO operates without inter-user interference, focusing solely on the desired signal. The SINR is expressed as:

$$\text{SINR}_\kappa^\eta = \frac{P_\kappa^\eta \left| (\mathbf{h}_\kappa^\eta)^T \mathbf{w}_\kappa^\eta \right|^2}{\sigma^2}, \quad \sigma^2 = 1 \quad (3.5)$$

The beamforming weight for **MRT** is designed to maximize the received power of the desired signal and is calculated as:

$$\mathbf{w}_\kappa^\eta = \frac{\mathbf{h}_\kappa^\eta}{\|\mathbf{h}_\kappa^\eta\|} \quad (3.6)$$

In **SU-MIMO**, the focus is on enhancing the signal power received at the **UE** while ensuring efficient power usage at the **BS**. The absence of intra-cell interference simplifies the processing and considers the individual user performance.

3.2.2 resource allocation

Thanks to its simplicity and flexibility, **Orthogonal Frequency Division Multiple Access (OFDMA)** is widely adopted as the standard multiple access scheme in **fourth generation (4G)** and **5G** cellular systems. In this scheme, the base station partitions the available frequency and time resources into **Physical Resource Block (PRB)**, which are then allocated dynamically to users. In this chapter, we will use **SU-MIMO** for legacy users, where we have one user assigned at each **PRB**. We have created a **SU-MIMO**, where each sub-channel has only one active user scheduled. The active user is assigned to each **PRB** separately based on **Exponential Moving Average (EMA)**. In addition, we will use equal power allocation, where each active user in the single **PRB** has equal power to the other users over a single timeslot per frame. The method used to calculate the spectral efficiency is **Modulation Coding Scheme (MCS)** from [26], and the system's performance metric is the geometric mean for all the users' throughput in the system.

Exponential Moving Average in Resource Allocation

In dynamic wireless communication systems, where network conditions and user demands fluctuate rapidly, using an **EMA** for **SINR** and throughput measurements is crucial for stabilizing resource allocation and scheduling decisions. The **EMA** for a user's throughput in each **PRB** and time slot is computed using the following formula:

$$R_u^{c,t} = \left(1 - \frac{1}{W}\right) \cdot R_u^{c,t-1} + \frac{1}{W} \cdot r_u^{c,t} \quad (3.7)$$

In equation 3.7, $R_u^{c,t}$ represents the updated EMA of the throughput for user u in PRB c at time slot t , while $R_u^{c,t-1}$ is the EMA of the throughput from the previous time slot. The term $r_u^{c,t}$ denotes the actual measured throughput for user u in PRB c at time slot t . The parameter W is the window size of the EMA, influencing how responsive the average is to recent changes in throughput.

Initialization and Weighted Rate Computation

At the start of each time slot, especially if it is the initial slot for a PRB in a new cycle, the EMA is set to a small constant ϵ (e.g., 1×10^{-10}). This constant helps avoid division by zero in rate calculations and ensures a baseline for the average to build upon. The weighted rate, important for PRB allocation decisions in EMA, is calculated in equation 3.8.

$$\text{Weighted Rate}_u = \frac{\text{Measured Throughput}_u}{R_u^{c,t-1}} \quad (3.8)$$

Calculating the Performance

Once the SINR is obtained, the MCS function is employed to calculate the throughput for the single user. Since SU-MIMO systems handle one user at a time, performance is primarily determined by the quality of the channel and the choice of the antenna tilt angle. Poor tilting configurations will reduce the throughput. Furthermore, the antenna tilt angle performance is based on the average geometric mean over several realizations or iterations in a single run or simulation.

3.3 Mechanical and Electrical tilt in SU-MIMO

We will test the effect and difference between mechanical and electrical tilt for 50 different realizations in SU-MIMO case with ULA and UPA system.

3.3.1 ULA antenna system with mechanical and electrical tilt

In this part, we have simulated 20 ground users for 50 realizations in SU-MIMO with ULA antenna system. Figure 3.2 and 3.3 show that mechanical tilt is better than electrical by 3.6 %. The best mechanical tilt in 3.2 is 9° with the best throughput of 72.2 Mbps, while the best electrical tilt in figure 3.3 is 10° with the best throughput of 69.7 Mbps. Moreover, figure 3.2 and 3.3 shows the angles that are above the threshold, where the threshold represents the range of angles that gives 95% of the maximum throughput.

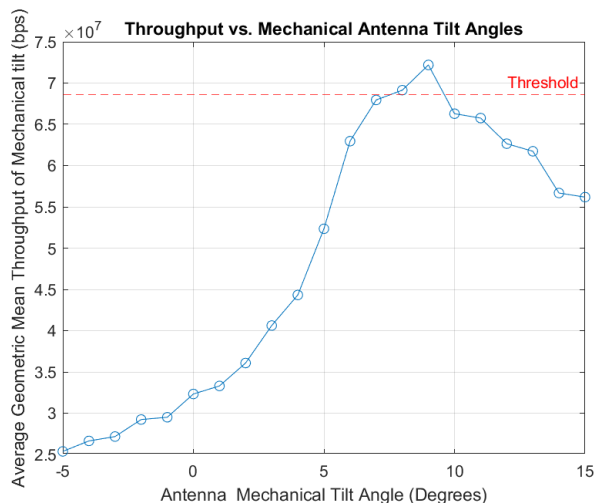


Figure 3.2: Throughput vs mechanical tilt in SU-MIMO

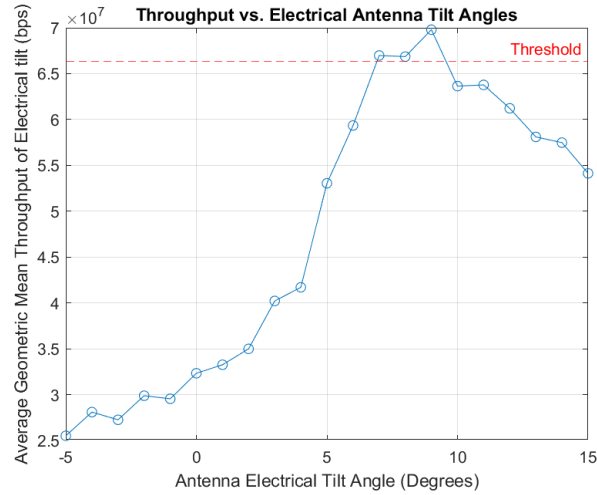


Figure 3.3: Throughput vs Electrical tilt in SU-MIMO

3.3.2 UPA antenna system with mechanical and electrical tilt

For this part, we did the same case from section 3.3.1 except we will use UPA antenna system. Figure 3.4 shows the best mechanical tilting angle is 14° with 44.7 Mbps, and figure 3.5 shows the best electrical tilting angle is also 14° with 44 Mbps. Moreover, ULA antenna system offers more throughput for users than UPA antenna system. The reason will be discussed in 3.3.3. The results in figure 3.4 and 3.5 shows that UPA antenna system needs more tilting unlike in ULA antenna system.

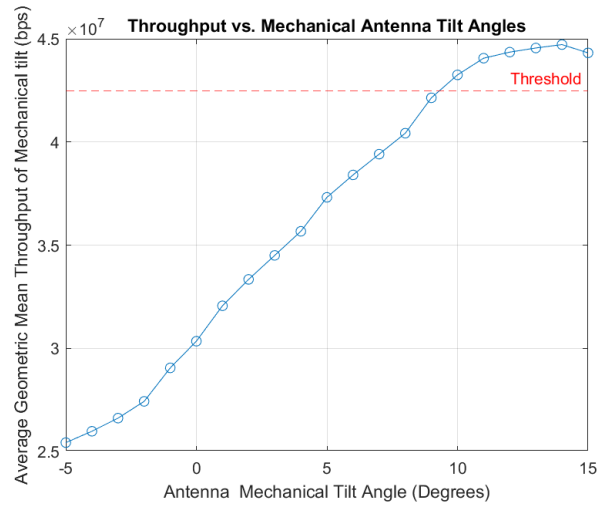


Figure 3.4: Throughput vs mechanical tilt in SU-MIMO in UPA system

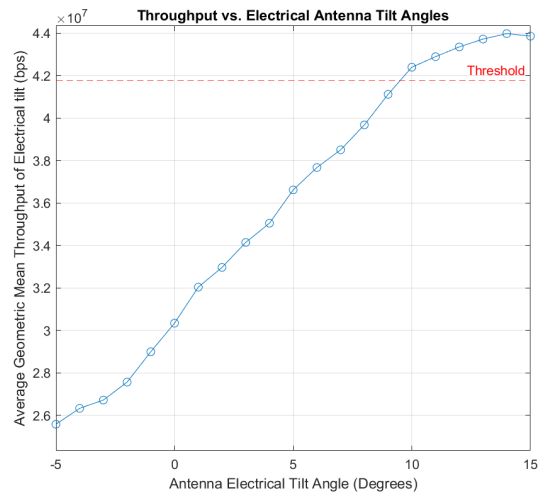


Figure 3.5: Throughput vs Electrical tilt in SU-MIMO in UPA system

Figure 3.6 shows the locations of ground users in the system in the UPA system.

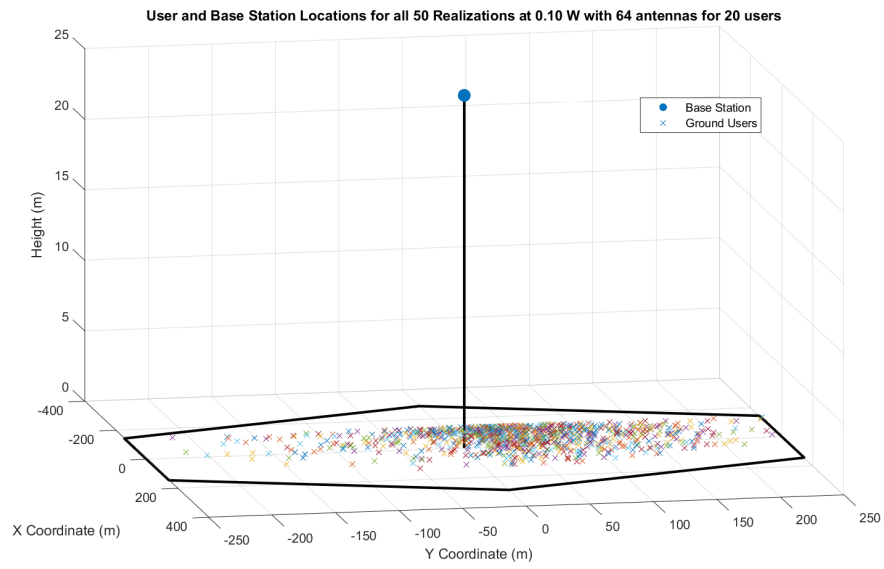


Figure 3.6: Location of the ground users in SU-MIMO with 20 ground users in UPA system

3.3.3 Difference between UPA and ULA in azimuth angle

Since many users have different locations, the azimuth would be different for each user, causing users with an azimuth angle above 0° to gain less due to the effect of horizontal antenna gain on the vertical antenna gain. The gain UPA at an azimuth angle of 45° would be less than the gain of ULA due to the sidelobes of horizontal gain as shown in the figure 3.7 :

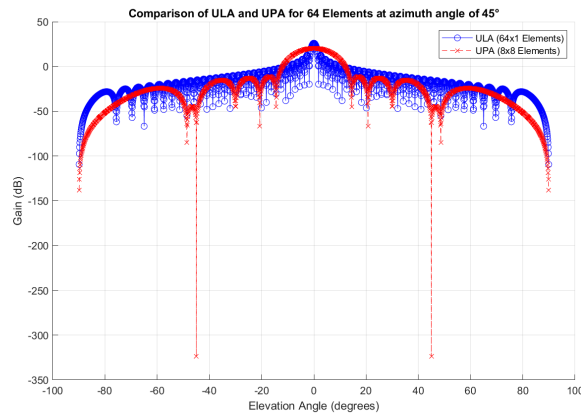


Figure 3.7: ULA Vs. UPA with 64 antenna elements in elevation angle at azimuth angle of 45°

If some users' locations are between 70° and 90° in terms of azimuth plane or angle, the UPA's gain would be less than the ULA's gain as shown in figure 3.8 :

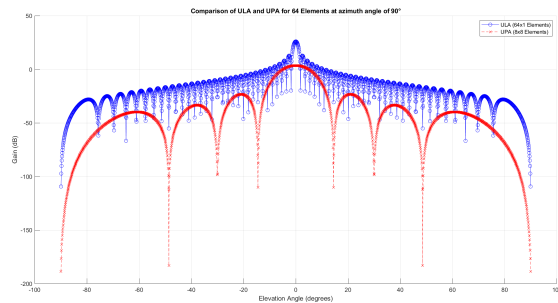


Figure 3.8: ULA Vs. UPA with 64 antenna elements in elevation angle at azimuth angle of 90°

3.4 Hybrid Tilting for Ground Users

As illustrated in section 2.1.3, electrical and mechanical tilting angles are separated tilting angles. In sections 3.4.1 and 3.4.2, we will show the difference between UPA and ULA systems in terms of hybrid tilting for 50 realizations. We will use different electrical and mechanical combinations ranging from -5° to 15° for both tilting in SU-MIMO ground users with BS's maximum power of 0.1W in later sections. Moreover, we will show and use the optimal tilting angles that give more than 95 % of the maximum throughput for ground users, and the optimal angles are described as any angle above the threshold.

3.4.1 Hybrid Tilting in ULA

Hybrid tilting in a ULA system combines both mechanical and electrical tilts by adding the respective tilt angles θ_m (mechanical tilt) and θ_e (electrical tilt). Equation 3.9 describes the antenna gain with hybrid tilting, and equation 3.10 shows the array factor with hybrid tilting.

$$G_{E,V}(\theta) = 8 - \min \left(12 \left(\frac{\theta - \theta_m}{HPBW_v} \right)^2, G_m \right), \quad \text{Hybrid-tilt Element Antenna Gain} \quad (3.9)$$

In equation 3.9, $G_{E,V}(\theta)$ represents the vertical element antenna gain in dB, while θ is the elevation angle of the incoming wave. The parameter θ_m denotes the mechanical tilt angle, $HPBW_v$ refers to the vertical half-power beamwidth (3 dB beamwidth), and G_m is the maximum allowable gain or the maximum attenuation of the antenna's gain (e.g., 30 dB as per 3GPP standards). The array factor for hybrid tilting, considering the combination of mechanical and electrical tilts, is described as:

$$A_f(\theta) = \frac{1}{\sqrt{N}} \times \frac{\sin \left(\frac{N\pi}{2} (\sin(\theta - \theta_m)) - \sin(\theta_e) \right)}{\sin \left(\frac{\pi}{2} (\sin(\theta - \theta_m)) - \sin(\theta_e) \right)}, \quad \text{Hybrid-tilt Array Factor} \quad (3.10)$$

Here, $A_f(\theta)$ is the array factor for the ULA considering hybrid tilting. The term N indicates the number of antenna elements in the ULA, while θ is the elevation angle. The parameters θ_m and θ_e correspond to the mechanical and electrical tilt angles.

The array factor gain, calculated from the magnitude of the array factor, is expressed as:

$$G_f(\theta) = 10 \log_{10} (A_f(\theta))^2, \quad \text{Array Factor Gain} \quad (3.11)$$

In this equation, $G_f(\theta)$ represents the gain contributed by the array factor in dB, while $A_f(\theta)$ is the array factor obtained from equation 3.10.

Finally, the total ULA gain, which combines the element gain and the array factor gain, is given by:

$$G_{\text{total}}(\theta) = G_e(\theta) + G_f(\theta), \quad \text{Total ULA Gain} \quad (3.12)$$

The term $G_{\text{total}}(\theta)$ refers to the total gain of the ULA in dB, where $G_e(\theta)$ is the element antenna gain from equation 3.9 and $G_f(\theta)$ is the array factor gain from equation 3.11. This comprehensive hybrid tilting model accurately represents the total gain for a ULA system by considering both mechanical and electrical tilts simultaneously.

Based on figure 3.9, the best tilting for the main lobe or gain beam is mechanical tilting, while the two hybrid tilting methods perform better than electrical tilting.

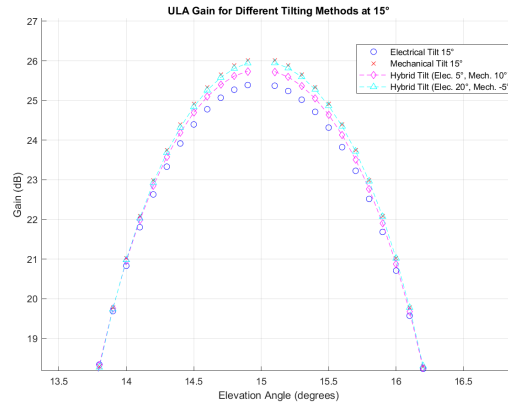


Figure 3.9: Gain(dB) vs Elevation Angle(°) with different tilting types at main beam

Based on the sidelobe's Gain in figure 3.10, hybrid tilting is the best type for maximizing sidelobe gain compared to mechanical tilting. Later, This will show how hybrid tilting is essential in future chapters for legacy UEs and cellular-connected UAVs.

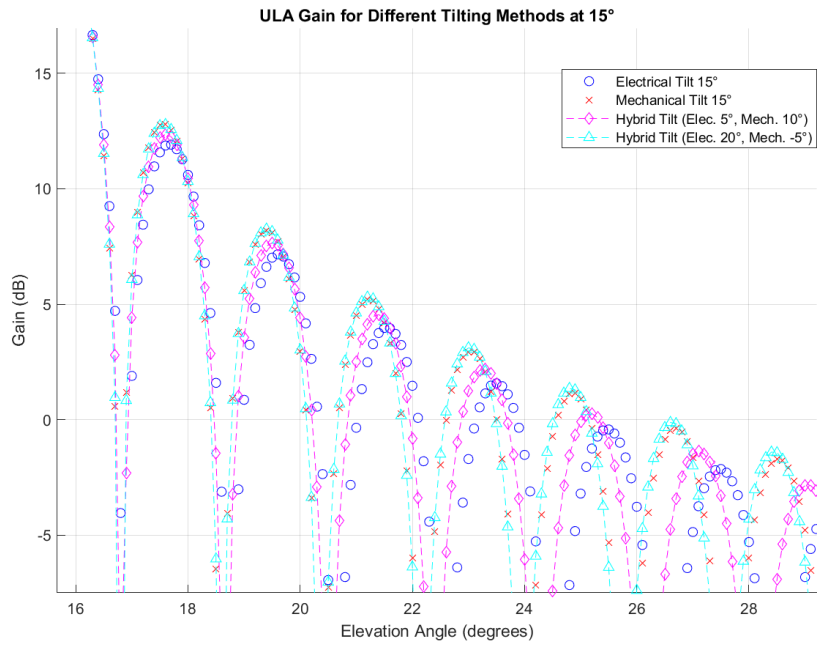


Figure 3.10: Gain(dB) vs Elevation Angle(°) with different tilting types at sidelobes

3.4.2 Hybrid tilting in UPA

Similar to section 3.4.1, we will just add element gain and array factor of the horizontal plane for a UPA antenna system.

Horizontal Gain equation in UPA

Element Gain in the Horizontal Plane: The element gain in the horizontal plane is given by:

$$G_H(\phi) = -\min\left(12\left(\frac{\phi}{\phi_{3dB}}\right)^2, G_h\right) \quad (3.13)$$

Where ϕ represents the azimuth angle of the antenna, ϕ_{3dB} is the half-power beamwidth (HPBW) in the horizontal plane, and G_h denotes the sidelobe level from 3GPP [14] for horizontal gain element.

Array Factor in the Horizontal Plane: The array factor in the horizontal plane for a uniform linear array (ULA) can be expressed as:

$$A_h = \frac{1}{\sqrt{N_2}} \cdot \frac{\sin\left(\frac{N_2\pi}{2}(\sin(\phi)\cos(\theta - \theta_m))\right)}{\sin\left(\frac{\pi}{2}(\sin(\phi)\cos(\theta - \theta_m))\right)} \quad (3.14)$$

Where N_2 represents the number of antenna elements in the horizontal ULA, θ denotes the elevation angle, and θ_m corresponds to the mechanical tilt.

Power of the Array Factor: The power of the array factor in the horizontal plane is calculated as:

$$G_h(\theta, \phi) = 10 \log_{10} \left((A_h(\theta, \phi))^2 \right) \quad (3.15)$$

Final Gain Calculation for Uniform Planar Array (UPA)

Total Gain Element: The total gain element for the uniform planar array (UPA) is computed as:

$$G_G(\theta, \phi) = 8 - \min\left(-(G_V + G_H), G_{max}\right) \quad (3.16)$$

Where G_V is the vertical element gain, G_H is the horizontal element gain, and G_{max} is the maximum allowed gain.

Final Array Factor: The final array factor, combining the horizontal and vertical contributions, is given by:

$$A_{\text{final}}(\theta, \phi) = (A_h)^2 \cdot (A_f)^2 \quad (3.17)$$

Final Gain from Array Factor: The Gain from the array factor is expressed as:

$$G_{\text{final}}(\theta, \phi) = 10 \log_{10}(A_{\text{final}}) \quad (3.18)$$

Total Gain: The total Gain, incorporating both element gains and the array factor, is calculated as:

$$\text{Total Gain}(\theta, \phi) = G_{\text{final}}(\theta, \phi) + G_G(\theta, \phi) \quad (3.19)$$

Figure 3.11 shows the difference between mechanical, electrical, and hybrid tilt at 15° shift in UPA system regarding gain beam pattern.

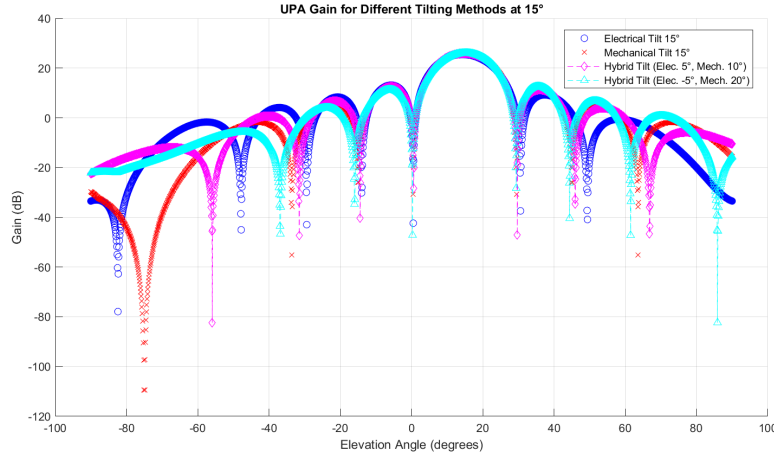


Figure 3.11: Gain(dB) vs Elevation Angle(°) with different tilting types

Figure 3.12 shows how Hybrid tilting is better than electrical tilt at the main beam lobe of UPA at 15° in terms of gain.

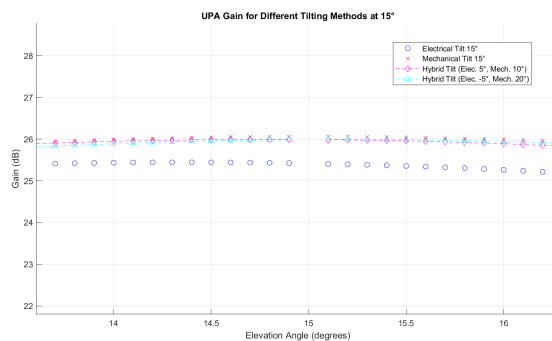


Figure 3.12: Gain(dB) vs Elevation Angle(°) with different tilting types at main beam

Similarly, in ULA, hybrid tilting is the best tilting for sidelobes in a UPA system. However, UPA has fewer sidelobes than ULA based on figure 3.13.

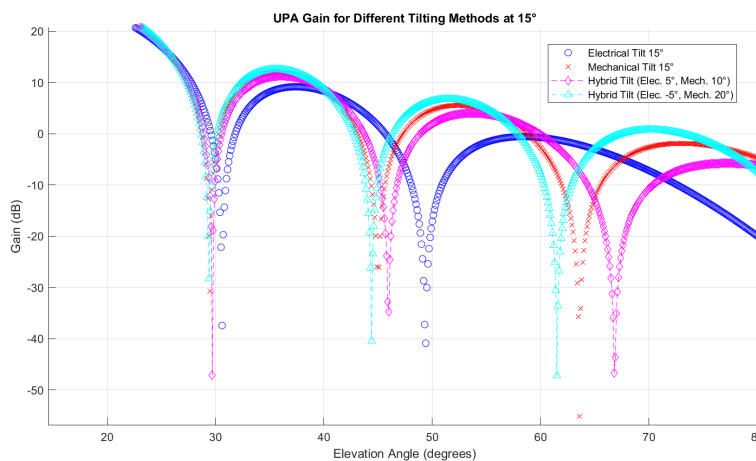


Figure 3.13: Gain(dB) vs Elevation Angle(°) with different tilting types at sidelobes in UPA

3.4.3 Hybrid tilting for ground users with ULA antenna system

Since we have done mechanical and electrical tilt in section 3.3.1 for ground users, we will use hybrid tilting for 20 ground users in SU-MIMO system. The best mechanical and electrical tilt for 20 ground users based on figure 3.14 is 12° and -3° , respectively. Moreover, the highest throughput in this part is 72.48 (Mbps) achieved by hybrid tilting. Figure 3.14 shows the Average geometric mean of 20 ground users with different hybrid tilting angles, where many different hybrid tilting angles are above the threshold that offers above 95% of the maximum geometric mean throughput of the ground users in the system. Table 3.2 shows the hybrid tilting, electrical, and mechanical tilt angles at the threshold and above with their respective throughput. Ground users have multiple hybrid tilting angles more than mechanical and electrical tilting within the 95% range based on table 3.2. Based on the results, hybrid tilting is slightly better than the best mechanical tilting in the ULA system in terms of average geometric mean throughput, and it's better than the best electrical tilting angle in the ULA system by 6.7%.

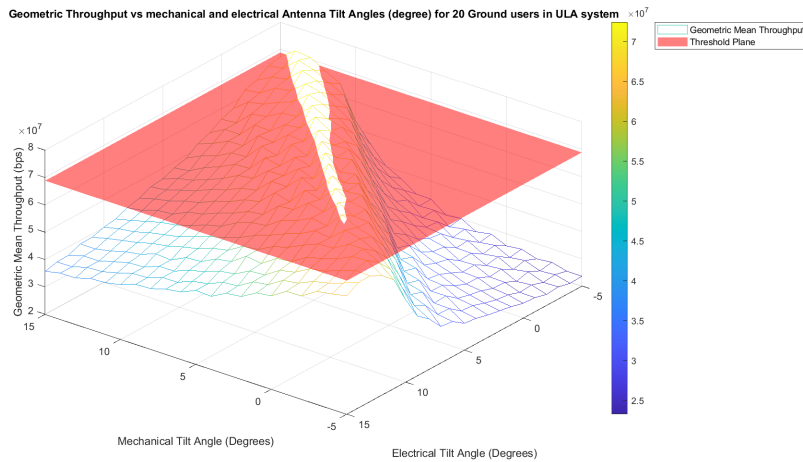


Figure 3.14: Throughput (bps) vs Hybrid tilt ($^\circ$) in ULA

Table 3.2: Optimal tilting angles for the geometric mean of ground users' throughput

Electrical Tilt (deg)	Mechanical Tilt (deg)	Throughput (Mbps)
-5.0	13.0	70.63
-5.0	14.0	71.33
-4.0	12.0	70.27
-4.0	13.0	72.01
-3.0	11.0	70.44
-4.0	10.0	72.98
-2.0	10.0	70.53
-2.0	11.0	71.72
-1.0	9.0	70.16
-1.0	10.0	72.02
0.0	8.0	69.14
0.0	9.0	72.20
1.0	7.0	68.88
1.0	8.0	72.08
2.0	7.0	71.44
3.0	6.0	71.56
4.0	5.0	71.57
5.0	4.0	71.75
6.0	3.0	71.53
7.0	2.0	71.07
8.0	1.0	69.99
9.0	0.0	69.79

3.4.4 Hybrid tilting for ground users with UPA antenna system

For UPA system, the results in the figure 3.15 and table 3.3 show that the maximum throughput is less than the maximum throughput in ULA antenna system in Figure 3.14 and table 3.2, and more hybrid tilting angles are needed in UPA system than in ULA system. The maximum throughput achieved for 20 ground users in UPA system is 44.9 (Mbps) with a mechanical tilt of 10° and an electrical tilt of 4° shown in red color in table 3.3. The reason why ground users in UPA antenna system achieve less throughput than in ULA antenna system is due to having different azimuth angles for each user in the system, which will decrease the overall antenna gain because of the horizontal gain antenna as mentioned in part 3.3.3. Overall, hybrid tilting is slightly better than mechanical and electrical tilting in UPA.

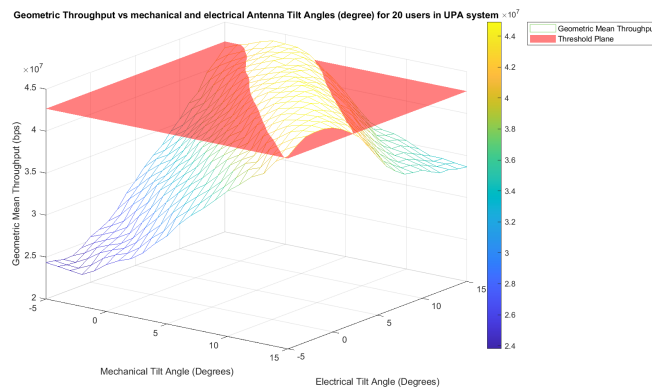


Figure 3.15: Throughput (bps) vs Hybrid tilt (°) in UPA

Table 3.3: Optimal tilting angles for geometric mean of ground users' throughput (Mbps) in UPA antenna system

Electrical tilt (deg)	Mechanical tilt (deg)	Throughput (Mbps)
-4.0000	11.0000	43.7024
-4.0000	13.0000	43.6997
-4.0000	15.0000	43.7911
-3.0000	11.0000	43.8162
-3.0000	13.0000	43.8200
-3.0000	15.0000	43.8406
-2.0000	11.0000	43.8481
-2.0000	13.0000	43.8479
-2.0000	15.0000	44.0555
-1.0000	11.0000	44.0724
-1.0000	13.0000	44.0724
-1.0000	15.0000	44.3827
0.0000	11.0000	44.6524
0.0000	13.0000	44.3655
0.0000	15.0000	45.2298
0.0000	17.0000	44.8000
0.0000	19.0000	44.3241
0.0000	21.0000	44.5546
0.0000	23.0000	44.7794
0.0000	25.0000	44.3383
0.0000	27.0000	43.1354
0.0000	29.0000	44.0480
0.0000	31.0000	44.2864
0.0000	33.0000	44.3646
0.0000	35.0000	44.0584
0.0000	37.0000	44.3105
0.0000	39.0000	43.7327
0.0000	41.0000	43.8162
0.0000	43.0000	44.0014
0.0000	45.0000	44.2724
0.0000	47.0000	44.7429
0.0000	49.0000	44.7239
0.0000	51.0000	44.3230
0.0000	53.0000	43.7942
0.0000	55.0000	42.3394
0.0000	57.0000	42.9322
0.0000	59.0000	43.3653
0.0000	61.0000	44.0623
0.0000	63.0000	44.7911
0.0000	65.0000	44.6326
0.0000	67.0000	44.2915
0.0000	69.0000	43.6465
0.0000	71.0000	43.3939
0.0000	73.0000	42.3396
0.0000	75.0000	43.8400
0.0000	77.0000	44.2861
0.0000	79.0000	44.7333
0.0000	81.0000	44.4934
0.0000	83.0000	43.7399
0.0000	85.0000	42.6696
0.0000	87.0000	42.9281
0.0000	89.0000	43.3535
0.0000	91.0000	44.0442
0.0000	93.0000	44.7624
0.0000	95.0000	43.7481
0.0000	97.0000	42.9822
0.0000	99.0000	42.3620
0.0000	101.0000	43.0523
0.0000	103.0000	44.3624
0.0000	105.0000	44.6302
0.0000	107.0000	43.8620
0.0000	109.0000	43.0446
0.0000	111.0000	42.7232
0.0000	113.0000	43.4406
0.0000	115.0000	43.8374
0.0000	117.0000	44.4244
0.0000	119.0000	44.8964
0.0000	121.0000	44.4862
0.0000	123.0000	43.7323
0.0000	125.0000	42.8123
0.0000	127.0000	43.2077
0.0000	129.0000	43.7395
0.0000	131.0000	43.3022
0.0000	133.0000	42.9823
0.0000	135.0000	44.0525
0.0000	137.0000	44.7748
0.0000	139.0000	43.3285
0.0000	141.0000	43.0823
0.0000	143.0000	43.3622
0.0000	145.0000	44.0000
0.0000	147.0000	44.8006
0.0000	149.0000	44.0611
0.0000	151.0000	43.7605
0.0000	153.0000	42.3642
0.0000	155.0000	43.0317
0.0000	157.0000	43.1390
0.0000	159.0000	44.0121
0.0000	161.0000	44.0763
0.0000	163.0000	44.3405
0.0000	165.0000	43.6090
0.0000	167.0000	42.9662
0.0000	169.0000	42.8099
0.0000	171.0000	43.2147
0.0000	173.0000	44.0829
0.0000	175.0000	43.8664
0.0000	177.0000	44.0325
0.0000	179.0000	43.4779
0.0000	181.0000	42.9805
0.0000	183.0000	42.6626
0.0000	185.0000	43.3495
0.0000	187.0000	43.0580
0.0000	189.0000	43.4400
0.0000	191.0000	44.1765
0.0000	193.0000	43.7676
0.0000	195.0000	43.0201
0.0000	197.0000	43.3443
0.0000	199.0000	43.7177
0.0000	201.0000	43.3623
0.0000	203.0000	44.1729
0.0000	205.0000	43.0127
0.0000	207.0000	43.1134
0.0000	209.0000	43.0628
0.0000	211.0000	43.4369
0.0000	213.0000	43.0822
0.0000	215.0000	43.3943
0.0000	217.0000	43.4754
0.0000	219.0000	43.3360
0.0000	221.0000	42.7399
0.0000	223.0000	43.5470
0.0000	225.0000	43.2821
0.0000	227.0000	43.8270
0.0000	229.0000	43.7610
0.0000	231.0000	43.1644

Chapter 4

Integrating UAVs in a legacy system with antenna tilt effect

Cellular-connected UAVs are integrated into the legacy system to observe how the impact of electrical, mechanical, or hybrid settings can affect the overall system for legacy users and UAV-UE. The following section will discuss the importance of having UAVs in the legacy system and its challenges and requirements. In addition, we will use the same system's setting from Chapter 3 for SU-MIMO system in this chapter.

4.1 The importance of UAVs in a legacy network system

UAVs have important roles in our daily lives. In this section, we will show different applications of UAVs that can be used as cellular-connected drones in the legacy system and types of UAV and challenges for it.

4.1.1 Types of UAVs

The application of UAVs determines the class of UAV. It is essential to implement the suitable UAV for any legacy or wireless system to be compatible with the cellular system. There are two distinct categories for UAVs, based on their altitude capabilities and the nature or mechanism of drones.

The two types of UAV based on their altitude [5] :

- **High altitude platforms (HAPs)** are UAVs or aerial vehicles deployed at high altitudes at 17 km and above, where these aerial vehicles stay more extended time at the stratosphere layer. Aircraft, airplanes, and balloons can be considered as HAPs. One example for HAPs would be an airplane that offloads its data with the BS at the airport [27]. HAPs can provide internet or cellular connectivity to rural or disaster-affected areas.
- **Low altitude platforms (LAPs)** are drones that operate in a wireless system at heights between a few meters and 10 km. LAPs have more probability of LOS, which helps enhance the cellular communication.

The two types of UAV based on the flight mechanism [5] :

- **Rotary-wing drones** are used in civil and commercial applications, where they are stationary and Quadcopter drones, and they are used for packing and surveillance. They are mainly used for wireless communication systems.
- **Fixed-wing drones** are usually much more robust than other drones but are faster and have high agility or motion. Fixed-wing drones have a higher probability of handover with ground BS due to their high movement and speed.

4.1.2 Applications of UAVs

UAVs have different applications that can improve the work for civil matters. In addition, each application has a different environment, objectives, and challenges. Figure 4.1 summarizes the various applications for UAVs [28].

1. Search and Rescue (SAR)

The objective of SAR is to find victims lost in a disaster by increasing the coverage of the affected areas. The UAVs are used to locate multiple or single victims on a disaster site, and the victims can be stationary or mobile [29]. There are several metrics to apply SAR. One of the benchmarks is the delay in response time of UAV [28]. The UAVs locate the victims and inform the authorities of the victims' location. The response of UAVs in a rescue mission is a crucial part of the mission of UAV

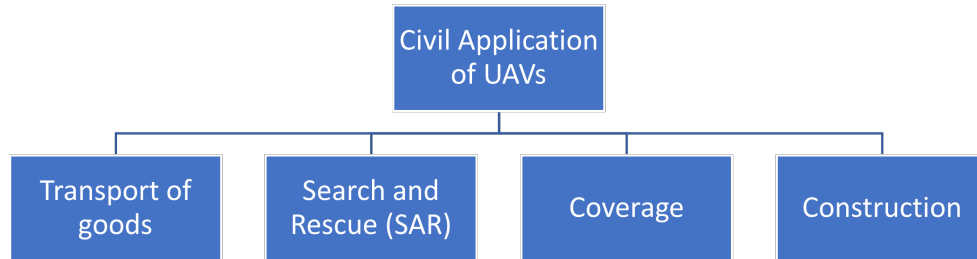


Figure 4.1: Different Applications of UAVs

in SAR, so any delay would be the death of a victim in a disaster. There are many challenges or constraints regarding SAR. The limited bandwidth can be a massive obstacle for SAR drones in the event of a disaster, and this will cause delay for SAR [28]. The number of victims and UAVs will increase the delay and put more constraints on the system. One of the ways to reduce delay in decision-making regarding SAR for drones is by utilizing the decentralized system for multiple UAVs [30]. However, the centralized method for SAR drones with known knowledge of the area can reduce cost, and it is much simpler than the decentralized method [31].

2. Coverage

Regarding coverage, the UAVs can serve many different applications for coverage, such as monitoring, surveillance, network coverage, and mapping. So, UAVs can be used as a relay in the legacy network [28]. To ensure continuous connectivity, multi-hop communication [32] or a delay-tolerant network [33] can be used for a system. Constant or periodic connectivity in drone area coverage is considered a constraint. Another challenge is the limited bandwidth for a system with many clients [28]. The main aim of coverage and surveillance is to provide reliability and stability in the system [34], and UAVs need to have an ideal relationship between different BSs [35]. Forest fire detection needs real-life monitoring and mapping application [36], and a system of UAVs with different roles and capacities is built to identify, confirm, localize, and monitor wildfires [28]. Two types of mission and control autonomy approaches are centralized and decentralized, similar to the methodology used in

SAR [36]. Moreover, UAVs can be used as the infrastructure of the legacy network, where this requires a decentralized method for UAVs [37]. In summary, monitoring and mapping handle critical data from the system or area, while tracking and event detection are handled by surveillance, and communication between ground UEs are managed by network coverage [28].

3. Construction

Drones can be used for construction sites to lift heavy weights from buildings and position them on the site. In addition, this will reduce the cost and be effective for construction projects [38]. The UAVs requirement on the construction site would be to get the building layout as data, which requires constant synchronization with the other UAVs. Moreover, Real-time synchronization is considered a challenge for drone workers on the construction site, and information must be provided to drones by a ground site BS, and ground stations are used to communicate to drones on the site for details on building sequencing on the construction site [39]. Collision avoidance, trajectory planning, location, synchronizations, and coordination are essential components that should be considered for UAV in the construction application. Furthermore, UAV can be categorized based on the payload of the building blocks or the task for the construction site, and the payload can be of light or heavy weight [28].

4. Transport of goods

Recently, UAVs are being used by both significant package delivery corporations like Amazon [40] and startups like Matternet [41] to expedite the delivery of medications and small supplies during disasters. One of the challenges UAV has in delivering is the longevity of the battery since long distances drain the battery much faster than other activities, and a reliable infrastructure is needed to store products and replace the battery UAV. To efficiently transfer products, drones require regular connection to the ground BS and GPS tracking [28]. A transportation system needs certain features for drones to deliver packages smoothly, such as collision avoidance, obstacle detection, and precision landing. Another consideration in the system or infrastructure would be the distance between the pick-up and delivery points. Moreover, the drone needs to have LOS component to maintain a connection with the ground BS for any information update [42]. Two methods are used for decision-making in delivery drones: centralized and decentralized, as mentioned previously for other UAVs applications. A decentralized method can be used when numerous UAVs need to

coordinate for joint load carrying and cannot communicate or connect directly with the ground station [42].

4.1.3 The communication links of UAVs

For any connectivity between UAVs and BS, there are two types of traffic channels which are [43] :

- Data Traffic encompasses various types of information, such as sensor data collected by UAVs, images, and real-time video streams.
- Command and Control (C&C) Traffic consists of telemetry data, real-time piloting, identity verification, authentication, and trajectory updates. It requires stringent Quality-of-Service (QoS) standards, particularly regarding reliability and low latency.

4.1.4 Challenges for UAVs

The antenna tilt angle can be used to solve some challenges related to cellular-connected UAVs in academia and industry, such as:

- Downlink transmission interference: Downlink transmission interference occurs when cellular-connected UAVs, flying at 100 meters, receive signals from BSs up to 10 kilometers away. This results in significant interference from multiple BSs, reducing the SINR for UAV-UEs compared to ground users [44].
- Uplink transmission interference: Cellular infrastructure assessments show that UAV-UEs face interference in uplink transmissions due to receiving LOS signals from multiple BSs as altitude increases. This interference, caused when UAV-UEs transmit to their serving BS, can disrupt the uplink connections of ground users with non-LoS transmissions [45].
- Association: UAV-UEs connect to cellular base stations through the sidelobes of their down-tilted antennas. Often, they establish links with base stations further away instead of the nearest one due to weak signals from nearby BSs. As a result of antenna pattern nulls and significant interference, UAV-UEs are more prone to handover failures and outages compared to ground users [46].

4.2 Cellular-connected UAV's setting

The cellular-connected UAV have their path-loss model and probability of LOS based on 3GPP [13]. In urban wireless communication environments, the propagation of signals is significantly influenced by the presence or absence of direct LOS between transmitters and receivers. This feature becomes particularly important for aerial vehicles due to their varying altitudes.

Rician factor for UAV

In studying wireless communication channels, particularly those involving UAV, the Rician K factor plays a role. This factor measures the dominance of the LOS path relative to other multi-path components. It is mathematically defined as:

$$K_i(t) = \lambda_1 e^{\lambda_2 \Theta'_i(t)}, \quad (4.1)$$

Where λ_1 and λ_2 are environmental coefficients that account for the specific propagation conditions of the environment [47], and $\Theta'_i(t)$ is the elevation angle. The elevation angle is crucial as it captures the angular relationship between the UAV and the ground station, affecting the line-of-sight component of the signal. For cellular-connected UAV, the channel model is being represented as a Rician fading model as mentioned in chapter 3 for ground UEs [48] :

$$\mathbf{g}_k^n = \sqrt{\frac{\beta_k^n}{1 + \kappa_k^n}} \mathbf{h}_G^n \mathbf{R}^{\frac{1}{2}} + \sqrt{\frac{\kappa_k^n \beta_k^n}{1 + \kappa_k^n}} \mathbf{h}_k^{\text{LOS},n} \quad (4.2)$$

Probability of LOS for UAVs

In urban environments, the probability of LOS is effective to aerial communication systems' performance. The 3GPP standard provides a model to estimate this probability, especially for UAVs operating within UMa environments. Based on 3GPP standard for UAVs in [13], cellular-connected UAV's has a higher probability of LOS than the ground user's probability of LOS at high altitudes. This shows that UAVs often have better throughput than ground users due to high probability of LOS.

4.3 Single-user MIMO with UAVs

To understand the factors that affect mechanical tilting in ULA antenna system on cellular-connected UAVs and ground users in a legacy system, we have created a SU-MIMO, where each sub-channel has only one active user scheduled. The active user is assigned to each PRB separately based on EMA. The method used to calculate the spectral efficiency is MCS from [26], and the system’s performance metric is the geometric mean. We used mechanical tilting in this section since mechanical tilting has a more significant effect than electrical tilting, as illustrated in section 3.3.

4.3.1 Power and Antenna tilting angle

In this part, we have simulated a system based on SU-MIMO with 100 realizations to test the effect of power on the antenna tilting angle in the legacy system, where the number of cellular-connected UAVs changes in each realization, and the ground user or UAV-UE, are generated randomly in a uniform fashion. Table 4.1 shows how increasing the maximum power of the BS requires less mechanical tilting for overall users in the system. Figures 4.2, 4.3, and 4.4 show the effect of power on the mechanical tilting for the ground users. The UAVs have higher throughput than ground users due to the high probability of LOS.

Table 4.1: Different power cases of 0.1,1, and 40W for 20 users with corresponding best tilting angle

Power	User Type	Tilt Angle (degrees)
0.1W	Ground Users	10
	UAV Users	-4
	All Users	10
1W	Ground Users	8
	UAV Users	-4
	All Users	7
40W	Ground Users	5
	UAV Users	-4
	All Users	6

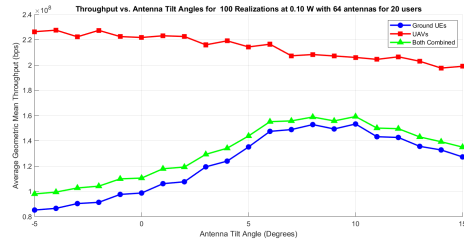


Figure 4.2: Throughput (bps) Vs Antenna tilt angles (degree) for 100 realizations with BS power of 0.1 W

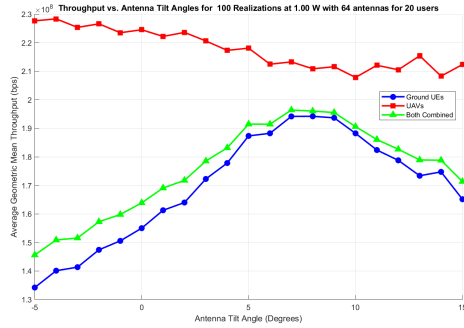


Figure 4.3: Throughput (bps) Vs Antenna tilt angles (degree) for 100 realizations with BS power of 1 W

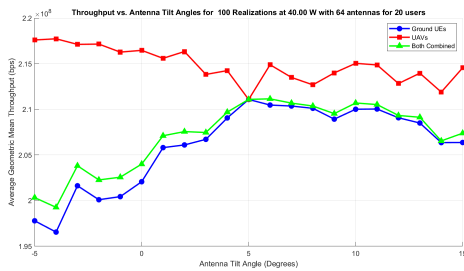


Figure 4.4: Throughput (bps) Vs Antenna tilt angles (degree) for 100 realizations with BS power of 40 W

4.3.2 Number of users case and antenna tilting angle

In this case, we change the number of users from 20 to 60 users, which consists of ground users with cellular-connected UAVs in a BS system with a maximum power of 0.1 W to observe any prominent change of tilting angle in SU-MIMO. Table 4.2 shows how the number of users can influence the best tilting if it reaches 40 users. However, 40 and 60 users have the same tilting angle in the case of the ground users' best mechanical tilting angle, as shown in table 4.2. Moreover, the more users we have, the less mechanical tiling is needed in the system based on the case of 20 and 40 users.

Table 4.2: Different numbers of users such as 20,40, and 60 at 0.1 W with corresponding best tilting angle.

Number of users	User Type	Tilt Angle (degrees)
20	Ground Users	10
	UAV Users	-4
	All Users	10
40	Ground Users	8
	UAV Users	-4
	All Users	8
60	Ground Users	8
	UAV Users	-4
	All Users	8

4.3.3 Number of Antenna and antenna tilting angle

To understand if the number of antennas has any significance on the tilting angle in the system, we have changed the number of antennas from 32 to 64 antenna elements in a system with legacy users and cellular-connected UAVs. Table 4.3 shows how fewer antennas require more tilting for ground users, as expected.

Table 4.3: 60 User with different numbers of antennas such as 32 and 64 at 0.1 W with corresponding best tilting angle

Number of Antennas	User Type	Tilt Angle (degrees)
32	Ground Users	8
	UAV Users	-5
	All Users	8
64	Ground Users	7
	UAV Users	-4
	All Users	7

4.4 Hybrid Tilting for Cellular-connected UAVs

Since we have done hybrid tilting for ground users in section 3.4, we can integrate cellular-connected UAVs with ground users with the same settings in chapter 3.

4.4.1 ULA system and Hybrid tilting

As mentioned in section 3.4.1, the ULA system has only vertical gain. We have simulated a SU-MIMO system with 20 UAVs and 20 ground UEs with 50 realizations as shown in figure 4.9, where the results show the performance with electrical and mechanical tilting in 3D. Based on section 3.4.1, hybrid tilting offers better gain at the sidelobes, and the results from table 4.4 show that hybrid tilting is the best tilting angle for ground users, drones, and overall users. The following figures represent the 3D throughput data for 20 users under different conditions: the first figure 4.5 shows the throughput for 20 ground users, the second figure 4.6 illustrates the throughput for 20 UAV users, the third figure 4.7 displays the throughput for 20 ground users with an applied threshold that depends on the maximum throughput as mentioned before, and fourth figure 4.8 shows how hybrid tilting angles give high throughput for UAVs and ground UEs combined geometric mean throughput.

Table 4.4: Best antenna hybrid tilt angles for different users in ULA

Run	User Type	Mechanical Tilt Angle (degrees)	Electrical Tilt Angle (degrees)	Geometric Mean Throughput (Mbps)
1	Ground Users	13	-5	29.2
	UAV Users	-5	-4	39.77
	All Users	3	5	26.93

The throughput of the UAVs using optimal tilting angles of the ground UEs is 22.1 Mbps, while the throughput of the ground UEs using optimal tilting angles of UAVs is 9.30 Mbps. To maintain the throughput of ground users with cellular-connected UAVs' throughput, we will use the optimal tilting angles that are above the threshold to see the best UAVs throughput, and these optimal angles offer the range within 95% of the maximum throughput of the ground users.

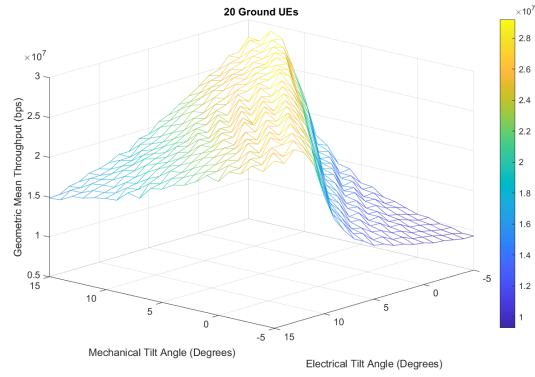


Figure 4.5: Throughput (bps) Vs Mechanical Antenna tilt angles (degree) vs electrical tilt (degree) for 20 ground UEs

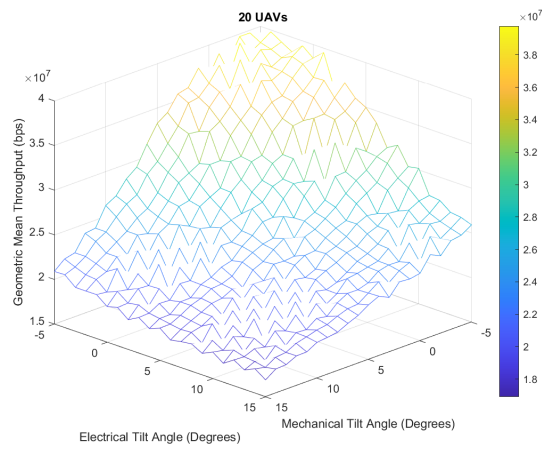


Figure 4.6: Throughput (bps) Vs Mechanical Antenna tilt angles (degree) vs electrical tilt (degree) for 20 UAVs

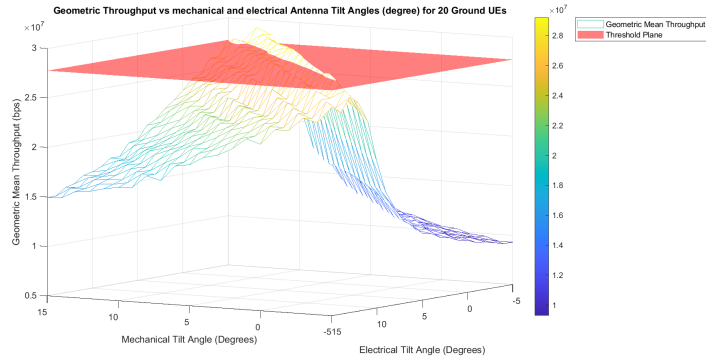


Figure 4.7: Throughput (bps) Vs Mechanical Antenna tilt angles (degree) vs electrical tilt (degree) for 20 ground UEs with threshold

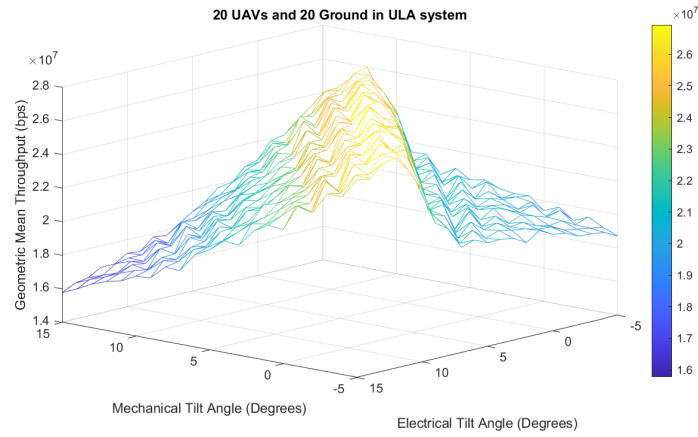


Figure 4.8: Throughput (bps) Vs Mechanical Antenna tilt angles (degree) vs electrical tilt (degree) for 20 ground UEs and 20 UAVs combined

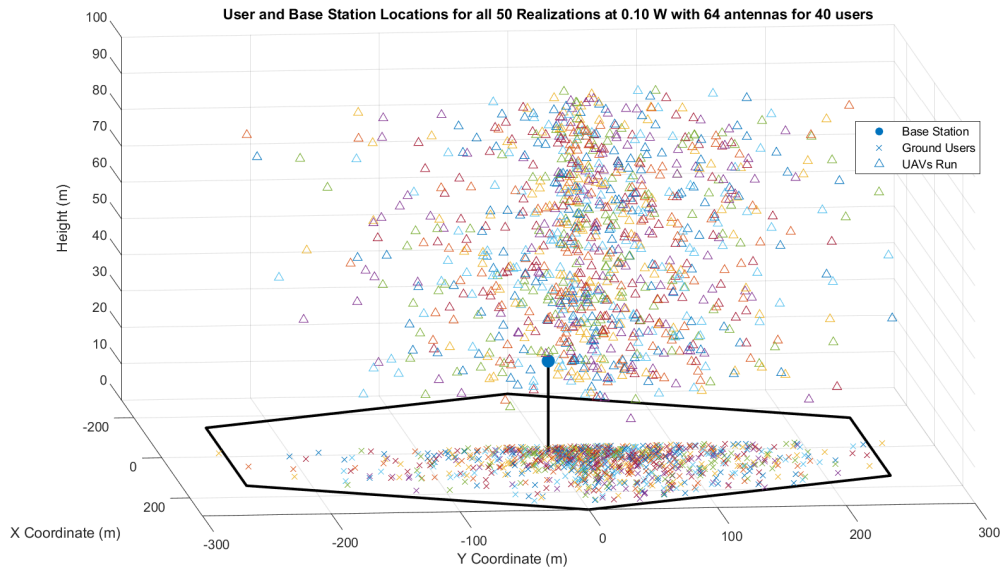


Figure 4.9: Location of the ground users in SU-MIMO with 20 ground users and 20 UAVs in ULA system

Based on table 4.5, the best tilting angle for ground users gives a throughput for UAVs by 22.144 Mbps, while the best tilting angle for UAVs using the optimal angle for ground users gives 26.382 Mbps. This shows an increase in throughput by 19.14% for UAVs. Hybrid tilting offers more throughput for UAVs than mechanical tilting by 4.65% in table 4.5. Moreover, hybrid tilting is better for UAVs than electrical tilting by 3%.

Table 4.5: Best hybrid tilting angles for ground UEs with UAVs' throughput in ULA system

Electrical Tilt Angle (degrees)	Mechanical Tilt Angle (degrees)	Geometric Mean Throughput of UAVs (Mbps)
-5	12	23.908
-5	13	22.144
-5	15	20.888
-4	11	24.055
-4	12	23.406
-4	13	22.146
-4	14	21.379
-3	10	24.123
-3	11	23.346
-2	9	23.839
-2	10	24.111
-1	8	24.905
-1	9	24.224
0	7	24.653
0	8	25.210
0	9	22.710
1	6	24.519
1	7	24.783
2	6	24.881
3	5	24.530
4	4	25.513
5	3	26.100
6	2	25.591
7	1	25.849
8	0	25.620
9	-1	26.167
10	-2	26.382

4.4.2 Optimal hybrid tilting angle with optimal realizations in ULA system

We simulated different realizations where each we have two systems: the first system with 20 ground UEs and the second with 20 cellular-connected UAVs. Separating both users in different systems is to observe the best and optimal hybrid tilting in a pure case where UAVs doesn't influence the scheduling of the ground users or the power allocation. Based on table 4.6, the optimal number of realizations to reach the best-converged hybrid tilting is 550 realizations, and the best hybrid tilting is 14° mechanical tilt and -5° electrical tilt.

Table 4.6: Best hybrid angles and their respective realizations from 20 to 1000

Electrical Tilt (deg)	mechanical (deg)	Realizations
-2	11	20
-3	12	50
-3	12	100
-3	12	150
-5	13	200
-5	13	350
-3	12	450
-5	14	550
-5	14	650
-5	14	750
-5	14	850
-5	14	1000

Figure 4.10 shows the optimal realizations from 550 to 1000 realizations share the optimal hybrid angles that are above the threshold except for three optimal angles:

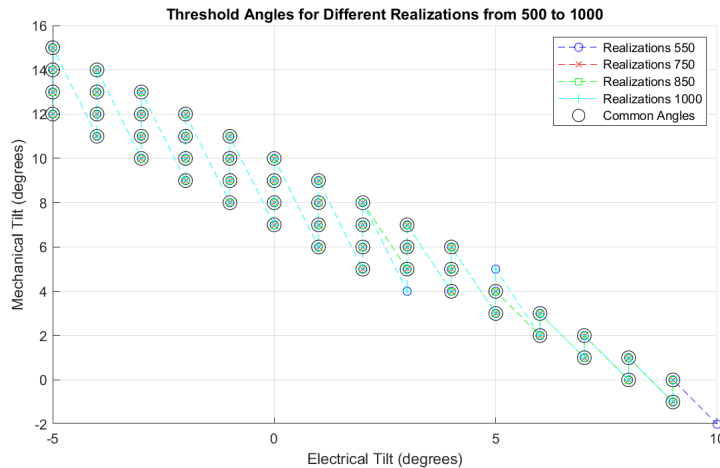


Figure 4.10: Common Tilting angle across different realizations between 500 and 1000

Since the optimal number of realizations is 550, the optimal tilting angles for ground users can be used to find the best down-tilted hybrid and non-hybrid tilting angles for cellular-connected UAVs as done before in table 4.5. Table 4.6 shows that the best and optimal hybrid tilting concerning ground UEs is 14° mechanical and -5° electrical tilt and the throughput for ground users is 76.71 Mbps with red color. In comparison, the throughput for UAVs in the same row is 54.1 Mbps, shown with the red color. The best tilting hybrid angle for UAVs within the 95% range for the ground users as discussed in section 4.4.1 is -2° mechanical and 10° electrical tilt and the throughput for UAVs is 64.9 Mbps. Furthermore, this shows that we can maintain 95% of the maximum throughput of the ground users and increase the UAVs' throughput by 20 % with optimal hybrid tilting. Moreover, hybrid tilting provides 5.5% throughput to UAV's than mechanical tilting (green color), and it is better than electrical tilting (blue color) by 3.17 % .

Table 4.7: UAV's and ground Users' throughput at different optimal down-tilted angles for 550 realizations in ULA system

Electrical Tilt (deg)	Mechanical Tilt (deg)	UAVs' Throughput (Mbps)	Ground UEs' Throughput (Mbps)
-5	12	57.7	69.74
-5	13	55.6	70.62
-5	14	54.1	76.71
-5	15	51.7	68.93
-4	11	59.9	69.39
-4	12	57.7	70.09
-4	13	55.8	70.56
-4	14	54.0	68.93
-3	10	59.8	69.30
-3	11	57.6	70.01
-3	12	55.8	70.68
-3	13	53.9	68.54
-2	9	60.4	68.93
-2	10	58.4	69.66
-2	11	57.0	70.43
-2	12	55.1	68.31
-1	8	61.4	68.50
-1	9	59.3	69.57
-1	10	57.1	70.01
-1	11	55.3	68.05
0	7	63.5	68.33
0	8	59.0	69.34
0	9	57.6	69.79
0	10	55.6	68.06
1	6	62.5	67.91
1	7	60.4	69.10
1	8	59.4	69.51
1	9	57.2	68.01
2	5	62.3	67.30
2	6	60.5	68.99
2	7	58.8	69.29
2	8	56.6	67.97
3	4	63.9	67.20
3	5	61.8	68.56
3	6	60.2	68.88
3	7	58.3	67.62
4	4	62.2	68.35
4	5	59.9	68.58
4	6	58.4	67.49
5	3	62.7	68.13
5	4	61.2	68.55
5	5	59.8	67.28
6	2	63.5	67.94
6	3	61.6	68.47
7	1	63.6	67.65
7	2	62.1	68.04
8	1	62.1	67.49
8	1	62.1	67.82
9	-1	64.7	67.26
9	0	62.9	67.54
10	-2	64.9	67.18

4.4.3 UPA system and hybrid tilting

In UPA system, we add horizontal gain as shown in section 2.1.2. Similarly, in section 4.4.1, the system has 20 ground users and 20 UAVs for 50 realizations. Table 4.8 shows how hybrid tilting angles offers the best throughput for ground users, cellular-connected UAVs, and overall users in the UPA antenna system.

Table 4.8: Best antenna hybrid tilt angles for different users in UPA

Run	User Type	Mechanical Tilt Angle (degrees)	Electrical Tilt Angle (degrees)	Geometric Mean Throughput (Mbps)
1	Ground Users	5	9	10.977
	UAV Users	-5	-5	18.149
	All Users	5	11	11.26

Figure 4.11 show how different hybrid tilting angles give high throughput for 20 ground users from table 4.8, while figure 4.12 also shows how hybrid tilting angles gives high throughput for 20 cellular-connected UAVs. In addition, the overall average geometric mean for all users consists of 20 ground users and 20 UAVs with different hybrid tilting angles as shown in figure 4.13. Figure 4.14 shows the throughput with hybrid tilting angles for 20 ground users with the threshold or range that gives 95% of the maximum throughput and above. Consequently, UPA system has more hybrid tilting angles within the achievable range of 95% of the maximum throughput of the ground users than ULA antenna system based on figure 4.7 and figure 4.14.

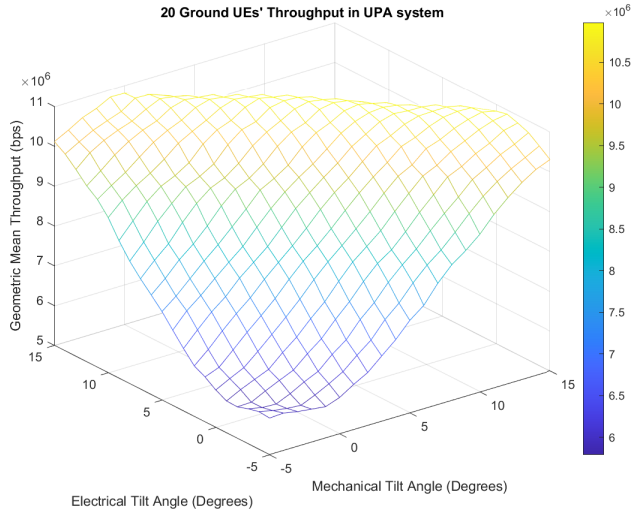


Figure 4.11: Throughput (bps) Vs Mechanical Antenna tilt angles (degree) vs electrical tilt (degree) for 20 ground UEs

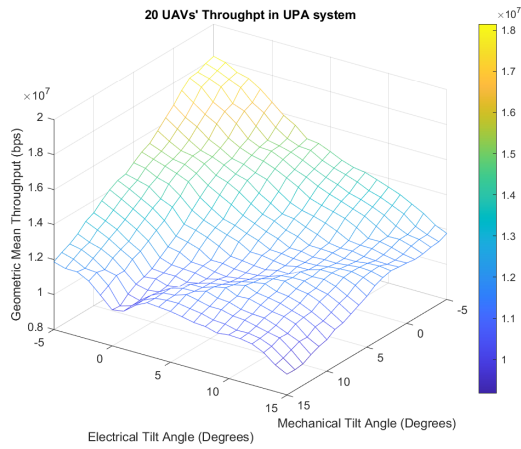


Figure 4.12: Throughput (bps) Vs Mechanical Antenna tilt angles (degree) vs electrical tilt (degree) for 20 UAVs

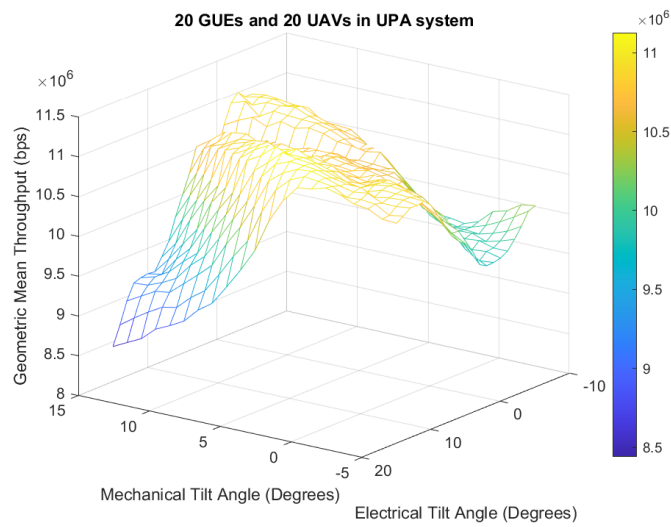


Figure 4.13: Throughput (bps) Vs Mechanical Antenna tilt angles (degree) vs electrical tilt (degree) for 40 UEs

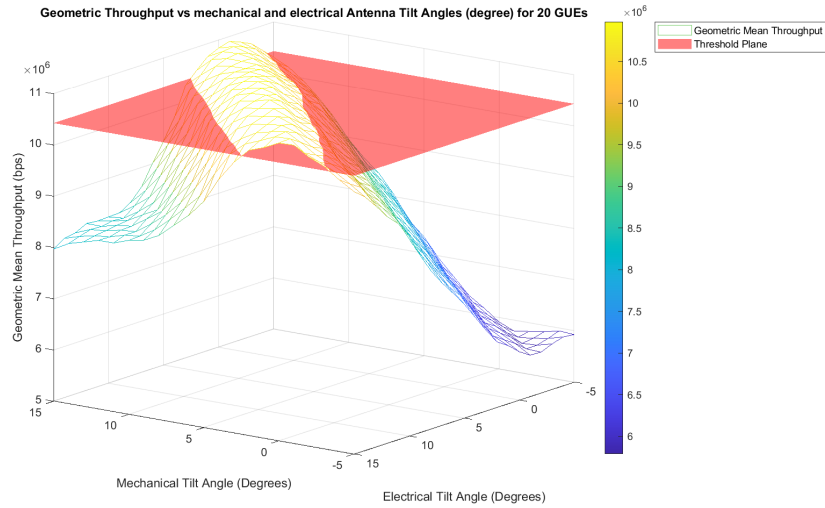


Figure 4.14: Throughput (bps) Vs Mechanical Antenna tilt angles (degree) vs electrical tilt (degree) for 20 UEs ground users with threshold

The reason why ground UEs have less throughput in UPA, based on table 4.4 and 4.8 system, is that users have different azimuth angles, which causes lower gain. Furthermore, cellular-connected UAVs have less throughput in UPA due to having sidelobes, as shown in figure 2.11. To have high throughput for ground users in UPA, the ground users need an azimuth angle around zero based on figure 2.11. Table 4.9 shows the throughput for ground users with an azimuth angle close to zero. The throughput of the ground users with azimuth angle around zero in table 4.9 is higher than the throughput of the ground users in table 4.8.

Table 4.9: Best antenna hybrid tilt angles for different users in UPA with azimuth angle of 0°

Run	User Type	Mechanical Tilt Angle (degrees)	Electrical Tilt Angle (degrees)	Geometric Mean Throughput (Mbps)
1	Ground Users	12	-1	35.254
	UAV Users	-5	-4	16.744
	All Users	-5	-4	24.101

4.4.4 Optimal hybrid tilting angle with optimal realizations in UPA system

Similar to section 4.4.2, two systems are used for comparison; the first system consists of 20 ground users, and the second system consists of 20 UAVs. For UPA environment, we need 650 realizations to reach the best and steady state of hybrid tiling angle for ground users based on the table 4.10. In UPA system, the best tilting angle for UAV's by using the optimal range of tilting angles for ground users that gives 95% of the maximum throughput is 14° mechanical and -4° electrical tilt as shown in yellow color in table 4.11.

Based on table 4.11, if we compare the best tilting angle for ground users which is 14° of mechanical tilt and -1° of electrical tilt, as shown in red color, and the best tilting angle for UAVs using optimal tilting angle for ground users, as shown in yellow color, we will find that UAVs' throughput improves by 7.67% in UPA system with hybrid tilting. Hybrid tilting offers more throughput for UAVs compared to optimal mechanical tilting (green row) by 7.04 %. In addition from table 4.11, hybrid tilting gives higher throughput than electrical tilt (blue row) for UAVs in table 4.11 by 1.56%.

Table 4.10: Best tilting angles and their Respective realizations from 550 to 850

Electrical Tilt (deg)	mechanical (deg)	Realizations
-0	13	550
-1	14	650
-1	14	750
-1	14	850

Table 4.11: Optimal electrical and mechanical tilt angles with 650 realizations in UPA system

Electrical Tilt (deg)	Mechanical Tilt (deg)	Ground U.S. Throughput (Mbps)	UAV Throughput (Mbps)	UAV Throughput (Mbps)
-10	10.0	41.01	41.98	41.98
-10	10.0	41.81	41.29	41.29
-10	11.0	41.97	41.13	41.13
-10	14.0	42.80	40.30	40.30
-10	15.0	41.30	41.80	41.80
-10	12.0	41.94	41.32	41.32
-10	13.0	41.79	41.47	41.47
-10	14.0	41.23	41.98	41.98
-10	15.0	41.51	41.71	41.71
-10	11.0	41.87	41.52	41.52
-10	12.0	41.71	41.69	41.69
-10	13.0	41.18	42.17	42.17
-10	14.0	41.47	41.88	41.88
-10	15.0	41.82	41.27	41.27
0	0.0	42.09	42.24	42.24
0	1.0	41.88	41.27	41.27
0	2.0	41.49	41.87	41.87
0	3.0	41.21	42.12	42.12
0	4.0	41.74	41.55	41.55
0	5.0	41.79	41.51	41.51
0	6.0	41.54	42.14	42.14
0	7.0	41.99	41.19	41.19
0	8.0	41.45	41.72	41.72
0	9.0	41.42	41.75	41.75
0	10.0	41.23	41.98	41.98
0	11.0	41.80	41.41	41.41
0	12.0	41.28	42.00	42.00
0	13.0	41.90	41.38	41.38
0	14.0	41.98	41.34	41.34
0	15.0	41.76	41.55	41.55
0	0.0	42.54	41.35	41.35
0	1.0	41.94	42.04	42.04
0	2.0	41.49	42.22	42.22
0	3.0	41.11	42.60	42.60
0	4.0	41.38	42.01	42.01
0	5.0	41.90	41.69	41.69
0	6.0	41.92	41.36	41.36
0	7.0	41.74	41.51	41.51
0	8.0	41.30	42.32	42.32
0	9.0	41.84	41.79	41.79
0	10.0	41.84	41.79	41.79
0	11.0	41.35	42.61	42.61
0	12.0	41.38	42.59	42.59
0	13.0	41.17	42.80	42.80
0	14.0	41.75	42.28	42.28
0	15.0	41.72	41.55	41.55
0	0.0	41.45	41.87	41.87
0	1.0	41.07	42.36	42.36
0	2.0	41.51	42.10	42.10
0	3.0	41.33	42.68	42.68
0	4.0	41.14	42.86	42.86
0	5.0	41.19	42.74	42.74
0	6.0	41.20	42.35	42.35
0	7.0	41.89	41.75	41.75
0	8.0	41.88	41.25	41.25
0	9.0	41.26	42.85	42.85
0	10.0	41.11	42.91	42.91
0	11.0	41.73	42.88	42.88
0	12.0	41.07	42.79	42.79
0	13.0	41.63	41.14	41.14
0	14.0	41.27	41.84	41.84
0	15.0	41.79	41.49	41.49
0	0.0	41.09	41.92	41.92
0	1.0	41.19	41.13	41.13
0	2.0	41.07	41.22	41.22
0	3.0	41.08	41.27	41.27
0	4.0	41.48	41.41	41.41
0	5.0	41.05	41.80	41.80
0	6.0	41.05	41.80	41.80
0	7.0	41.11	41.24	41.24
0	8.0	41.06	41.32	41.32
0	9.0	41.05	41.37	41.37
0	10.0	41.96	41.31	41.31
0	11.0	41.13	41.51	41.51
0	12.0	41.27	41.36	41.36
0	13.0	41.07	41.56	41.56
0	14.0	41.07	41.56	41.56
0	15.0	41.07	41.67	41.67
0	0.0	41.93	41.54	41.54
0	1.0	41.37	41.63	41.63
0	2.0	41.95	41.53	41.53
0	3.0	41.37	41.63	41.63
0	4.0	41.07	41.91	41.91
0	5.0	41.04	41.30	41.30
0	6.0	41.81	41.55	41.55
0	7.0	41.96	41.36	41.36
0	8.0	41.04	41.14	41.14
0	9.0	41.25	41.32	41.32
0	10.0	41.22	41.65	41.65
0	11.0	41.51	41.65	41.65
0	12.0	41.84	41.69	41.69
0	13.0	41.04	41.14	41.14
0	14.0	41.25	41.32	41.32
0	15.0	41.22	41.65	41.65
0	0.0	42.84	41.46	41.46
0	1.0	41.97	41.42	41.42
0	2.0	42.52	41.31	41.31
0	3.0	41.97	41.29	41.29
0	4.0	41.97	41.98	41.98
0	5.0	41.24	41.51	41.51
0	6.0	41.71	41.21	41.21
0	7.0	41.97	41.70	41.70
0	8.0	41.96	41.29	41.29
0	9.0	41.94	41.30	41.30
0	10.0	41.94	41.30	41.30
0	11.0	41.94	41.30	41.30
0	12.0	41.94	41.30	41.30
0	13.0	41.94	41.30	41.30
0	14.0	41.94	41.30	41.30
0	15.0	41.94	41.30	41.30
0	0.0	41.94	41.30	41.30
0	1.0	41.94	41.30	41.30
0	2.0	41.94	41.30	41.30
0	3.0	41.94	41.30	41.30
0	4.0	41.94	41.30	41.30
0	5.0	41.94	41.30	41.30
0	6.0	41.94	41.30	41.30
0	7.0	41.94	41.30	41.30
0	8.0	41.94	41.30	41.30
0	9.0	41.94	41.30	41.30
0	10.0	41.94	41.30	41.30
0	11.0	41.94	41.30	41.30
0	12.0	41.94	41.30	41.30
0	13.0	41.94	41.30	41.30
0	14.0	41.94	41.30	41.30
0	15.0	41.94	41.30	41.30
0	0.0	41.94	41.30	41.30
0	1.0	41.94	41.30	41.30
0	2.0	41.94	41.30	41.30
0	3.0	41.94	41.30	41.30
0	4.0	41.94	41.30	41.30
0	5.0	41.94	41.30	41.30
0	6.0	41.94	41.30	41.30
0	7.0	41.94	41.30	41.30
0	8.0	41.94	41.30	41.30
0	9.0	41.94	41.30	41.30
0	10.0	41.94	41.30	41.30
0	11.0	41.94	41.30	41.30
0	12.0	41.94	41.30	41.30
0	13.0	41.94	41.30	41.30
0	14.0	41.94	41.30	41.30
0	15.0	41.94	41.30	41.30
0	0.0	41.94	41.30	41.30
0	1.0	41.94	41.30	41.30
0	2.0	41.94	41.30	41.30
0	3.0	41.94	41.30	41.30
0	4.0	41.94	41.30	41.30
0	5.0	41.94	41.30	41.30
0	6.0	41.94	41.30	41.30
0	7.0	41.94	41.30	41.30
0	8.0	41.94	41.30	41.30
0	9.0	41.94	41.30	41.30
0	10.0	41.94	41.30	41.30
0	11.0	41.94	41.30	41.30
0	12.0	41.94	41.30	41.30
0	13.0	41.94	41.30	41.30
0	14.0	41.94	41.30	41.30
0	15.0	41.94	41.30	41.30
0	0.0	41.94	41.30	41.30
0	1.0	41.94	41.30	41.30
0	2.0	41.94	41.30	41.30
0	3.0	41.94	41.30	41.30
0	4.0	41.94	41.30	41.30
0	5.0	41.94	41.30	41.30
0	6.0	41.94	41.30	41.30
0	7.0	41.94	41.30	41.30
0	8.0	41.94	41.30	41.30
0	9.0	41.94	41.30	41.30
0	10.0	41.94	41.30	41.30
0	11.0	41.94	41.30	41.30
0	12.0	41.94	41.30	41.30
0	13.0	41.94	41.30	41.30
0	14.0	41.94	41.30	41.30
0	15.0	41.94	41.30	41.30
0	0.0	41.94	41.30	41.30
0	1.0	41.94	41.30	41.30
0	2.0	41.94	41.30	41.30
0	3.0	41.94	41.30	41.30
0	4.0	41.94	41.30	41.30
0	5.0	41.94	41.30	41.30
0	6.0	41.94	41.30	41.30
0	7.0	41.94	41.30	41.30
0	8.0	41.94	41.30	41.30
0	9.0	41.94	41.30	41.30
0	10.0	41.94	41.30	41.30
0	11.0	41.94	41.30	41.30
0	12.0	41.94	41.30	41.30
0	13.0	41.94	41.30	41.30
0	14.0	41.94	41.30	41.30
0	15.0	41.94	41.30	41.30
0	0.0	41.94	41.30	41.30
0	1.0	41.94	41.30	41.30
0	2.0	41.94	41.30	41.30
0	3.0	41.94	41.30	41.30
0	4.0	41.94	41.30	41.30
0	5.0	41.94	41.30	41.30
0	6.0	41.94	41.30	41.30
0	7.0	41.94	41.30	41.30
0	8.0	41.94	41.30	41.30
0	9.0	41.94	41.30	41.30
0	10.0	41.94	41.30	41.30
0	11.0	41.94	41.30	41.30
0	12.0	41.94	41.30	41.30
0	13.0	41.94	41.30	41.30
0	14.0	41.94	41.30	41.30
0	15.0	41.94	41.30	41.30
0	0.0	41.94	41.30	41.30
0	1.0	41.94	41.30	41.30
0	2.0	41.94	41.30	41.30
0	3.0	41.94	41.30	41.30
0	4.0	41.94	41.30	41.30
0	5.0	41.94	41.30	41.30
0	6.0	41.94	41.30	41.30
0	7.0	41.94	41.30	41.30
0	8.0	41.94	41.30	41.30
0	9.0	41.94	41.30	41.30
0	10.0	41.94	41.30	41.30
0	11.0	41.94	41.30	41.30
0	12.0	41.94	41.30	41.30
0	13.0	41.94	41.30	41.30
0	14.0	41.94	41.30	41.30
0	15.0	41.94	41.30	41.30
0	0.0	41.94	41.30	41.30
0	1.0	41.94	41.30	41.30
0	2.0	41.94	41.30	41.30
0	3.0	41.94	41.30	41.30
0	4.0	41.94	41.30	41.30
0	5.0	41.94	41.30	41.30
0	6.0	41.94	41.30	41.30
0	7.0	41.94	41.30	41.30
0	8.0	41.94	41.30	41.30
0	9.0	41.94	41.30	41.30
0	10.0	41.94	41.30	41.30
0	11.0	41.94	41.30	41.30
0	12.0	41.94	41.30	41.30
0	13.0	41.94	41.30	41.30
0	14.0	41.94	41.30	41.30
0	15.0	41.94	41.30	41.30
0	0.0	41.94	41.30	41.30
0	1.0	41.94	41.30	41.30
0	2.0	41.94	41.30	41.30
0	3.0	41.94	41.30	41.30
0	4.0	41.94	41.30	41.30
0	5.0	41.94	41.30	41.30
0	6.0	41.94	41.30	41.30
0	7.0	41.94	41.30	41.30
0	8.0	41.94	41.30	41

Chapter 5

Conclusions

In this thesis, we illustrated the main difference between mechanical and electrical tilt using element gain and array factor gain for the legacy wireless network with its ground users and cellular-connected UAVs. In mechanical tilt, we physically change the position of the antenna's gain beam pattern by changing the elevation angle. In contrast, electrical tilt is done by changing the adjustment of the main beam of an antenna's radiation pattern by electronically controlling the signal's phase fed to each element in the antenna array without changing the physical aspect of the antenna in the BS. In addition, we used electrical and mechanical tilting angles simultaneously to show hybrid tilting, where hybrid tilting has significance for the sidelobes in ULA and UPA antenna systems.

Mechanical tilt provides better throughput for legacy users than electrical tilt by 5.6 % in ULA system. In contrast, mechanical tilt slightly improves in the UPA system compared to electrical tilt. Electrical tilt increases the throughput by 73.07 % in ULA system compared to a zero tilting angle system. Our study also showed how combined or hybrid tilting using optimal titling for ground users can increase the UAV's performance by 20% in a ULA system. Furthermore, hybrid tilting increased the UAV's throughput performance by 7.67%. Moreover, Hybrid tiling is better than mechanical tilting and electrical tilting in terms of throughput in ULA and UPA antenna systems.

Hybrid tilting raises further questions regarding its significance in a MU-MIMO and how it can be used in multi-BS systems with multiple sectors in each BS. Furthermore, more investigation needs to be done regarding hybrid tilting and its effect on the base station's association with cellular-connected UAVs and the use of dynamic optimization for hybrid tilting in a cellular network.

References

- [1] M. Asadpour, B. Van den Bergh, D. Giustiniano, K. A. Hummel, S. Pollin, and B. Plattner, “Micro aerial vehicle networks: An experimental analysis of challenges and opportunities,” *IEEE Communications Magazine*, vol. 52, no. 7, pp. 141–149, 2014.
- [2] F. A. Administration, “FAA Aerospace Forecast Fiscal Years 2022–2042,” https://www.faa.gov/sites/faa.gov/files/2022-06/Unmanned_Aircraft_Systems.pdf, 2022, [Accessed 11-September-2022].
- [3] G. Geraci, A. Garcia-Rodriguez, M. M. Azari, A. Lozano, M. Mezzavilla, S. Chatzino-tas, Y. Chen, S. Rangan, and M. Di Renzo, “What will the future of UAV cellular communications be? a flight from 5G to 6G,” *IEEE Communications Surveys & Tutorials*, vol. 24, no. 3, pp. 1304–1335, 2022.
- [4] T. Kim, S. Lee, K. H. Kim, and Y.-I. Jo, “FANET routing protocol analysis for multi-UAV-based reconnaissance mobility models,” *Drones*, vol. 7, no. 3, 2023. [Online]. Available: <https://www.mdpi.com/2504-446X/7/3/161>
- [5] M. Mozaffari, W. Saad, M. Bennis, Y.-H. Nam, and M. Debbah, “A tutorial on UAVs for wireless networks: Applications, challenges, and open problems,” *IEEE Communications Surveys & Tutorials*, vol. 21, no. 3, pp. 2334–2360, 2019.
- [6] B. Li, Z. Fei, and Y. Zhang, “UAV communications for 5G and beyond: Recent advances and future trends,” *IEEE Internet of Things Journal*, vol. 6, no. 2, pp. 2241–2263, 2019.
- [7] G. Geraci, A. Garcia-Rodriguez, L. G. Giordano, D. López-Pérez, and E. Björnson, “Understanding UAV cellular communications: From existing networks to massive MIMO,” *IEEE Access*, vol. 6, pp. 67 853–67 865, 2018.

- [8] D. Mishra and E. Natalizio, “A survey on cellular-connected uavs: Design challenges, enabling 5g/b5g innovations, and experimental advancements,” *Computer Networks*, vol. 182, p. 107451, 2020. [Online]. Available: <https://www.sciencedirect.com/science/article/pii/S1389128620311324>
- [9] A. Fakhreddine, C. Bettstetter, S. Hayat, R. Muzaffar, and D. Emini, “Handover challenges for cellular-connected drones,” in *Proceedings of the 5th Workshop on Micro Aerial Vehicle Networks, Systems, and Applications*, 2019, pp. 9–14.
- [10] R. Amer, W. Saad, and N. Marchetti, “Toward a connected sky: Performance of beamforming with down-tilted antennas for ground and uav user co-existence,” *IEEE Communications Letters*, vol. 23, no. 10, pp. 1840–1844, 2019.
- [11] A. Derneryd and M. Johansson, “Advanced antennas for radio base stations,” in *Antennas for Base Stations in Wireless Communications*, 1st ed., Z. N. Chen and K.-M. Luk, Eds. New York: McGraw-Hill, 2009, ch. 4. [Online]. Available: <https://www.accessengineeringlibrary.com/content/book/9780071612883/chapter/chapter4>
- [12] F. Athley and M. N. Johansson, “Impact of electrical and mechanical antenna tilt on LTE downlink system performance,” in *2010 IEEE 71st Vehicular Technology Conference*, 2010, pp. 1–5.
- [13] 5G Americas, “Study on enhanced LTE support for aerial vehicles,” Technical Specification Group Radio Access Network, Technical Report 3GPP TR 36.777, Dec. 2017.
- [14] 3GPP, “Study on channel model for frequencies from 0.5 to 100 ghz,” 3rd Generation Partnership Project (3GPP), Technical Report TR 38.901, 2020.
- [15] P. Butovitsch, E. Larsson, D. Astely, B. Göransson, A. Furuskar, B. Hogan, and J. Karlsson, *Advanced Antenna Systems for 5G Networks*. Stockholm, Sweden: Ericsson AB, Jun. 2020.
- [16] O. N. C. Yilmaz, S. Hamalainen, and J. Hamalainen, “Comparison of remote electrical and mechanical antenna downtilt performance for 3GPP LTE,” in *2009 IEEE 70th Vehicular Technology Conference Fall*, Anchorage, AK, USA, 2009, pp. 1–5.
- [17] N. Seifi, M. Coldrey, M. Matthaiou, and M. Viberg, “Impact of base station antenna tilt on the performance of network MIMO systems,” in *2012 IEEE 75th Vehicular Technology Conference (VTC Spring)*, Yokohama, Japan, 2012, pp. 1–5.

- [18] N. Dandanov, H. Al-Shatri, A. Klein *et al.*, “Dynamic self-optimization of the antenna tilt for best trade-off between coverage and capacity in mobile networks,” *Wireless Personal Communications*, vol. 92, no. 1, pp. 251–278, 2017. [Online]. Available: <https://doi.org/10.1007/s11277-016-3849-9>
- [19] M. M. U. Chowdhury, I. Guvenc, W. Saad, and A. Bhuyan, “Ensuring reliable connectivity to cellular-connected uavs with up-tilted antennas and interference coordination,” *arXiv preprint arXiv:2108.05090*, 2021. [Online]. Available: <https://arxiv.org/abs/2108.05090>
- [20] M. Lobão, W. Feitosa, R. Antonioli, Y. Silva, W. Jr, and G. Fodor, “On the impact of antenna tilt on cell-free systems serving ground users and uavs,” in *Proceedings of the 2023 Brazilian Symposium on Telecommunications and Signal Processing (SBrT)*, January 2023.
- [21] Y. Du, H. Zhang, and J. Peng, “Modeling and coverage analysis for cellular-connected UAVs with up-tilted antenna,” *IEEE Communications Letters*, vol. 26, no. 11, pp. 2572–2575, Nov 2022.
- [22] S. Kim, M. Kim, J. Y. Ryu, and J. Lee, “Impact of base station antenna tilt angle on UAV communications,” in *GLOBECOM 2020 - 2020 IEEE Global Communications Conference*, 2020, pp. 1–6.
- [23] X. Xu and Y. Zeng, “Cellular-connected UAV: Performance analysis with 3d antenna modelling,” in *2019 IEEE International Conference on Communications Workshops (ICC Workshops)*, 2019, pp. 1–6.
- [24] Y. Zhang, P. Mitran, and C. Rosenberg, “Joint resource allocation for linear precoding in downlink massive MIMO systems,” *IEEE Transactions on Communications*, vol. 69, no. 5, pp. 3039–3053, 2021.
- [25] D. Ying, F. W. Vook, T. A. Thomas, D. J. Love, and A. Ghosh, “Kronecker product correlation model and limited feedback codebook design in a 3d channel model,” in *Proceedings of the IEEE International Conference on Communications (ICC)*, June 2014, pp. 5865–5870.
- [26] A. Hussein, P. Mitran, and C. Rosenberg, “Operating multi-user massive MIMO networks: Trade-off between performance and runtime,” *IEEE Transactions on Network and Service Management*, vol. 21, no. 2, pp. 2170–2186, 2024.

- [27] A. Shaverdian, S. Shahsavari, and C. Rosenberg, “Air-to-ground cellular communications for airplane maintenance data offloading,” *IEEE Transactions on Vehicular Technology*, vol. 71, no. 10, pp. 11 060–11 077, 2022.
- [28] S. Hayat, E. Yanmaz, and R. Muzaffar, “Survey on unmanned aerial vehicle networks for civil applications: A communications viewpoint,” *IEEE Communications Surveys & Tutorials*, vol. 18, no. 4, pp. 2624–2661, 2016.
- [29] G. Chmaj and H. Selvaraj, “Distributed processing applications for UAV/drones: A survey,” in *Progress in Systems Engineering*, ser. Advances in Intelligent Systems and Computing. Cham, Switzerland: Springer, 2015, vol. 366, pp. 449–454.
- [30] D. J. Pack, P. DeLima, G. J. Toussaint, and G. York, “Cooperative control of UAVs for localization of intermittently emitting mobile targets,” *IEEE Transactions on Systems, Man, and Cybernetics, Part B (Cybernetics)*, vol. 39, no. 4, pp. 959–970, Aug. 2009.
- [31] M. A. Goodrich *et al.*, “Supporting wilderness search and rescue using a camera-equipped mini UAV,” *Journal of Field Robotics*, vol. 25, no. 1–2, pp. 89–110, 2008.
- [32] S. Morgenthaler, T. Braun, Z. Zhao, T. Staub, and M. Anwander, “UAVNet: A mobile wireless mesh network using unmanned aerial vehicles,” in *Proc. IEEE GLOBECOM Workshop-WiUAV*, 2012, pp. 1603–1608.
- [33] M. Asadpour, D. Giustiniano, K. A. Hummel, S. Heimlicher, and S. Egli, “Now or later? delaying data transfer in time-critical aerial communication,” in *Proc. ACM Conf. Emerg. Netw. Experiments Technol. (CoNEXT)*, 2013, pp. 127–132.
- [34] L. Reynaud, T. Rasheed, and S. Kandeepan, “An integrated aerial telecommunications network that supports emergency traffic,” in *Proc. Int. Symp. Wireless Pers. Multimedia Commun. (WPMC)*, Oct. 2011, pp. 1–5.
- [35] S. Srinivasan, H. Latchman, J. Shea, T. Wong, and J. McNair, “Airborne traffic surveillance systems: Video surveillance of highway traffic,” in *Proc. ACM Int. Workshop Video Surveillance Sensor Netw.*, 2004, pp. 131–135.
- [36] “COMETS Project,” <https://grvc.us.es/comets/>, 2002–2005, [Online; accessed July 16, 2024].
- [37] P. B. Charlesworth, “A non-cooperative game to coordinate the coverage of two communications UAVs,” in *Proc. IEEE Military Commun. Conf. (MILCOM)*, Nov. 2013, pp. 668–673.

- [38] J. Willmann *et al.*, “Aerial robotic construction towards a new field of architectural research,” *International Journal of Architectural Computing*, vol. 10, no. 3, pp. 439–460, 2012.
- [39] Q. Lindsey, D. Mellinger, and V. Kumar, “Construction with quadrotor teams,” *Autonomous Robots*, vol. 33, no. 3, pp. 323–336, 2012.
- [40] E. Ackerman, “Amazon promises package delivery by drone: Is it for real?” <https://spectrum.ieee.org/amazon-prime-air-package-drone-delivery>, 2013, accessed on Jun. 2024.
- [41] —, “Matternet wants to deliver meds with a network of quadrotors,” <https://spectrum.ieee.org/mini-uavs-could-be-the-cheapest-way-to-deliver-medicine>, Aug. 2011, accessed on Jun. 2024.
- [42] M. Cummings and A. Collins, “Autonomous aerial cargo/utility system (AA-CUS)—concept of operations,” Dept. Navy, Office Naval Research, Arlington, VA, USA, Tech. Rep. 12-004-CONOPS, 2011.
- [43] H. Nawaz, H. M. Ali, and A. A. Laghari, “UAV communication networks issues: A review,” *Archives of Computational Methods in Engineering*, vol. 28, no. 3, pp. 1349–1369, 2021.
- [44] R. Amorim, H. Nguyen, P. Mogensen, I. Z. Kovács, J. Wigard, and T. B. Sørensen, “Radio channel modeling for UAV communication over cellular networks,” *IEEE Wireless Communications Letters*, vol. 6, no. 4, pp. 514–517, 2017.
- [45] C. H. Liu, Z. Chen, J. Tang, J. Xu, and C. Piao, “Energy-efficient UAV control for effective and fair communication coverage: A deep reinforcement learning approach,” *IEEE Journal on Selected Areas in Communications*, vol. 36, no. 9, pp. 2059–2070, Sep. 2018.
- [46] B. Hu, H. Yang, L. Wang, and S. Chen, “A trajectory prediction based intelligent handover control method in UAV cellular networks,” *China Communications*, vol. 16, no. 1, pp. 1–14, 2019.
- [47] A. F. Mostafa, M. Abdel-Kader, Y. Gadallah, and O. Elayat, “Machine learning-based multi-uav deployment for uplink traffic sizing and offloading in cellular networks,” *IEEE Access*, vol. 11, pp. 71 314–71 325, 2023.

- [48] C. You and R. Zhang, “3d trajectory optimization in rician fading for UAV-enabled data harvesting,” *IEEE Transactions on Wireless Communications*, vol. 18, no. 6, pp. 3192–3207, 2019.
- [49] S. A. R. Naqvi, S. A. Hassan, H. Pervaiz, and Q. Ni, “Drone-aided communication as a key enabler for 5G and resilient public safety networks,” *IEEE Communications Magazine*, vol. 56, no. 1, pp. 36–42, 2018.
- [50] 5G Americas, “Study on enhanced lte support for aerial vehicles,” Technical Specification Group Radio Access Network, Technical Report 3GPP TR 36.777, Dec 2017.
- [51] R. Amer, W. Saad, and N. Marchetti, “Toward a connected sky: Performance of beamforming with down-tilted antennas for ground and uav user co-existence,” *IEEE Communications Letters*, vol. 23, no. 10, pp. 1840–1844, 2019.